

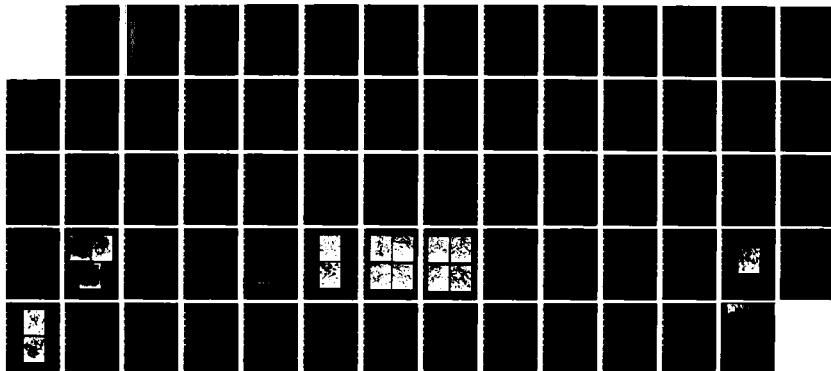
AD-A140 795

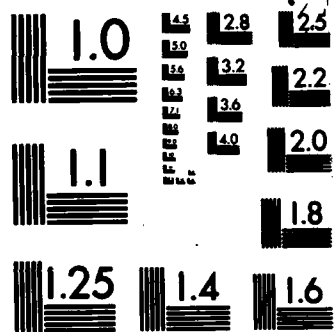
DEVELOPMENT OF SINTERED Si3N4 FOR HIGH PERFORMANCE  
THERMOMECHANICAL APPLI. (U) GENERAL ELECTRIC CORPORATE  
RESEARCH AND DEVELOPMENT SCHENECTA. W D PASCO JAN 84  
84SRD026 AMRC-TR-84-4 DAAG46-82-C-0053 F/G 13/8

1/1

UNCLASSIFIED

NL

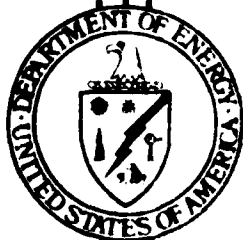




MICROCOPY RESOLUTION TEST CHART  
NATIONAL BUREAU OF STANDARDS-1963-A

ENERGY

DTIC FILE COPY ZOHKJH0Z00



AD-A140 795

AD

AD

AMMRC TR 84-4

DEVELOPMENT OF SINTERED Si<sub>3</sub>N<sub>4</sub> FOR HIGH PERFORMAN  
THERMOMECHANICAL APPLICATIONS

Wayne D. Pasco

January 1984

GENERAL ELECTRIC COMPANY  
CORPORATE RESEARCH AND DEVELOPMENT  
SCHENECTADY, NEW YORK 12301

Final Report - 30 August 1982 to 30 August 1983

Contract DAAG46-82-C-0053

Approved for public release; distribution unlimited.

Prepared for

ARMY MATERIALS AND MECHANICS RESEARCH CENTER  
Watertown, Massachusetts 02172

Under AMMRC/DOE Interagency Agreement EC-76-A-1017-002  
Department of Energy

Office of Vehicle and Engine Research and Development  
Ceramic Technology for Advanced Heat Engines Programs

DTIC  
ELECTE

MAY 4 1984

U. S. DEPARTMENT OF ENERGY

A

Office of Vehicle and Engine Research and Development

84 05 04 004

The findings in this report are not to be construed as an official Department of the Army position, unless so designated by other authorized documents.

Mention of any trade names or manufacturers in this report shall not be construed as advertising nor as an official endorsement or approval of such products or companies by the United States Government.

**DISPOSITION INSTRUCTIONS**

Destroy this report when it is no longer needed.  
Do not return it to the originator

REPORT DOCUMENTATION PAGE

|   |       |   |  |
|---|-------|---|--|
| 1a. REPORT SECURITY CLASSIFICATION<br><b>Unclassified</b>   |       | 1b. RESTRICTIVE MARKINGS  |  |
| 2a. SECURITY CLASSIFICATION AUTHORITY   |       | 3. DISTRIBUTION/AVAILABILITY OF REPORT<br><b>Approved for public release; distribution unlimited.</b>       |  |
| 2b. DECLASSIFICATION/DOWNGRADING SCHEDULE   |       |   |  |
| 4. PERFORMING ORGANIZATION REPORT NUMBER(S)<br><b>84SRD026</b>  |       | 5. MONITORING ORGANIZATION REPORT NUMBER(S)<br><b>AMMRC TR-84-4</b>   |  |
| 6a. NAME OF PERFORMING ORGANIZATION<br><b>General Electric Company<br/>Corporate Research and Development</b>   |       | 7a. NAME OF MONITORING ORGANIZATION<br><b>DCASMA Hartford</b>   |  |
| 6b. OFFICE SYMBOL<br><i>(If applicable)</i>   |       | 7b. ADDRESS (City, State and ZIP Code)<br><b>Hartford, CT 06114</b>   |  |
| 6c. ADDRESS (City, State and ZIP Code)<br><b>Schenectady, New York 12301</b>  |       | 7c. ADDRESS (City, State and ZIP Code)  |  |
| 8a. NAME OF FUNDING/SPONSORING ORGANIZATION<br><b>Army Materials and Mechanics Research Center</b>  |       | 9. PROCUREMENT INSTRUMENT IDENTIFICATION NUMBER<br><b>DAAG46-82-C-0053</b>                                  |  |
| 8b. OFFICE SYMBOL<br><i>(If applicable)</i>   |       | 10. SOURCE OF FUNDING NOS.  |  |
| 8c. ADDRESS (City, State and ZIP Code)<br><b>Attn: DRXMR-K<br/>Watertown, MA 021</b>  |       | PROGRAM ELEMENT NO. PROJECT NO. TASK NO. WORK UNIT NO.<br><b>Interagency Agreement<br/>EC-76-A-1017-002</b> |  |
| 11. TITLE <b>Development of Sintered Si<sub>3</sub>N<sub>4</sub> for High Performance Thermomechanical Applications</b>   |       |   |  |
| 12. PERSONAL AUTHOR(S) <b>Wayne D. Pasco</b>  |       |   |  |
| 13a. TYPE OF REPORT<br><b>Final Report</b>  |       | 13b. TIME COVERED<br><b>FROM 30 Aug. 1982 TO 30 Aug. 1983</b>   |  |
| 14. DATE OF REPORT (Yr., Mo., Day)<br><b>January 1984</b>   |       | 15. PAGE COUNT<br><b>56</b>   |  |
| 16. SUPPLEMENTARY NOTATION<br><b>1.7 X 10 to the -11 power sq. Kg/m to the -4 power / s      .005/h</b>   |       |   |  |
| 17. COSATI CODES  |       | 18. SUBJECT TERMS   |  |
| FIELD   | GROUP | SUB. GR.  | <b>Sintering<br/>Silicon nitrides<br/>Ceramics materials<br/>Beryllium compounds<br/>High temperature<br/>Yttrium oxides</b> |
|   |       |   |  |
| 19. ABSTRACT (Continue on reverse if necessary and identify by block number) <b>00004/h</b>   |       |   |  |
| <p><b>3/2 psu. r</b> The sintering of Si<sub>3</sub>N<sub>4</sub> containing BeSiN<sub>2</sub> and Y<sub>2</sub>O<sub>3</sub> was examined and found to yield densities greater than 99% on a routine basis. A composition containing 2.5 wt% BeSiN<sub>2</sub> and 3.0 wt% Y<sub>2</sub>O<sub>3</sub> displayed a room temperature strength of greater than 690 MPa and a fracture toughness K<sub>IC</sub> of about 6 MNm<sup>-3/2</sup>, a creep rate of 4 x 10<sup>-3</sup> h<sup>-1</sup> at 1300 °C under a 69 MPa load, and a parabolic rate constant for oxidation at 1350 °C of 1.5 x 10<sup>-11</sup> kg<sup>2</sup>m<sup>-4</sup>s<sup>-1</sup>. This composition has adequate properties for high temperature structural applications except for the high creep rate, which is of the same order as NC-132.</p> <p>The sintering of Si<sub>3</sub>N<sub>4</sub> containing 5 wt% LiAlO<sub>2</sub> and 3 wt% YF<sub>3</sub> was examined and found to yield densities of greater than 96%. The creep rate of this composition was 5 x 10<sup>-3</sup> h<sup>-1</sup> at 1300 °C under a 69 MPa load. The high creep rate, in conjunction with a moderately high oxidation rate, precludes the use of this composition for high temperature structural applications.</p> <p>A new source of Si<sub>3</sub>N<sub>4</sub> powder, made by Ube Industries, was qualified as an alternative powder source of this program. The addition of 7 wt% BeSiN<sub>2</sub> in conjunction with a total oxygen content of 3.5 wt% yielded sintered densities of greater than 98.5%.</p> |       |   |  |
| 20. DISTRIBUTION/AVAILABILITY OF ABSTRACT<br><b>UNCLASSIFIED/UNLIMITED</b> <input type="checkbox"/> SAME AS RPT. <input type="checkbox"/> DTIC USERS <input type="checkbox"/>   |       | 21. ABSTRACT SECURITY CLASSIFICATION<br><b>Unclassified</b>   |  |
| 22a. NAME OF RESPONSIBLE INDIVIDUAL<br><b>Wayne D. Pasco</b>  |       | 22b. TELEPHONE NUMBER<br><b>518*385-8180</b>  |  |
|   |       | 22c. OFFICE SYMBOL  |  |

## TABLE OF CONTENTS

|  | Page |
|--|------|
| List of Figures.....   | i    |
| List of Tables.....  | ii   |
| Foreword .....   | iii  |
| Summary of Important Results.....  | 1    |
| I. Introduction.....   | 2    |
| II. Scope of the Work.....   | 5    |
| III. Experimental Procedure.....   | 5    |
| A. Preparation of BeSiN <sub>2</sub> .....   | 5    |
| B. Preparation of Y <sub>2</sub> O <sub>3</sub> .....  | 6    |
| C. Preparation of LiAl <sub>5</sub> O <sub>8</sub> .....   | 6    |
| D. Batch Preparation for Initial Compositional Studies.....  | 6    |
| E. Batch Preparation of Optimized Compositions.....  | 7    |
| F. Powder Compaction.....  | 8    |
| IV. Sintering and Property Studies Using BeSiN <sub>2</sub> and Y <sub>2</sub> O <sub>3</sub> Additives.....                                       | 8    |
| A. Initial Sintering Studies Using BeSiN <sub>2</sub> and Y <sub>2</sub> O <sub>3</sub> Additives.....   | 8    |
| B. "Grain Boundary Composition" Study.....   | 10   |
| C. Optimization of the Sintering Process.....  | 12   |
| D. Properties of Si <sub>3</sub> N <sub>4</sub> Containing BeSiN <sub>2</sub> and Y <sub>2</sub> O <sub>3</sub> Additives.....                     | 12   |
| D.1 Room Temperature MOR.....  | 12   |
| D.2 Examination of Fracture Surfaces.....  | 13   |
| D.3 Creep.....   | 14   |
| D.4 Oxidation.....   | 16   |
| D.5 Vicker's Hardness and K <sub>IC</sub> Measurements.....  | 17   |
| E. Microstructural and Phase Characterization.....   | 17   |
| V. Sintering and Property Studies of Si <sub>3</sub> N <sub>4</sub> Containing LiAl <sub>5</sub> O <sub>8</sub> and YF <sub>3</sub> Additions..... | 19   |
| A. Sintering Studies.....  | 19   |
| B. Properties.....   | 20   |
| VI. Evaluation of Various Sintering Aids.....  | 21   |
| VII. Evaluation of Ube Si <sub>3</sub> N <sub>4</sub> Powder.....  | 21   |
| VIII. Conclusions.....   | 23   |
| IX. References.....  | 25   |
| X. Appendix A.....   | 51   |

## LIST OF FIGURES

|           | <u>Page</u>  |    |
|-----------|--|----|
| Figure 1  | Densification Behavior as a Function of Temperature for the (1.5,2), (2,2) and (3,2) Compositions.....   | 29 |
| Figure 2  | Densification Behavior as a Function of Temperature for the (1.5, 3) (2,3) and (3,3) Compositions.....   | 30 |
| Figure 3  | Fracture Surfaces of the (a) (2.5, 3) Composition, (b) (3,3) Composition, and (c) Baseline Composition.....  | 35 |
| Figure 4  | Oxidation Behavior of the (2.5, 3) (3,3) and Baseline Compositions at 1300°C in Flowing Oxygen.....  | 37 |
| Figure 5  | Oxidation Behavior of the (2.5,3) (3,3), Baseline and GTE Sylvania Compositions at 1350°C in Flow Oxygen.....  | 38 |
| Figure 6  | SEM Micrographs of Oxidized Surfaces of the (a) (2.5, 3) and (b) (3,3) Compositions.....   | 39 |
| Figure 7  | SEM Micrographs of Fracture Surfaces of (a) the (2.5, 3) Composition Fired at 2025°C (b) the (3,3) Composition Fired at 2025°C, (c) the (2.5, 3) Composition Fired at 2050°C, and (d) the (3,3) Composition Fired at 2050°C..... | 40 |
| Figure 8  | SEM Micrographs of Fracture Surface of (a) the (2,2) Composition (b) the (2.5, 2.5) Composition, (c) the (3,4) Composition and (d) the (4,3) Composition Fired at 2050°C.....  | 41 |
| Figure 9  | Plot of Be Solubility in $\beta$ -Si <sub>3</sub> N <sub>4</sub> versus Temperatures as Reported by Huseby et al <sup>(20)</sup> .....   | 43 |
| Figure 10 | SEM Micrograph of Fracture Surface Si <sub>3</sub> N <sub>4</sub> + 5 w/o LiAl <sub>5</sub> O <sub>8</sub> + 3 w/o YF <sub>3</sub> .....   | 46 |
| Figure 11 | SEM Micrograph Showing Particle Size and Morphology of (a) Ube Industries, Si <sub>3</sub> N <sub>4</sub> and GTE Sylvania SN502 in the As-received Condition.....   | 48 |

## LIST OF TABLES

|            |  | <u>Page</u> |
|------------|--|-------------|
| Table I    | Comparison of Properties of Small and Large Samples<br>of GPS $\text{Si}_3\text{N}_4$ .....  | 27          |
| Table II   | Sintering Behavior of $\text{Si}_3\text{N}_4$ Containing $\text{BeSiN}_2$ and<br>$\text{Y}_2\text{O}_3$ Additives.....   | 28          |
| Table III  | Weight Change During Sintering as a Function of Temperature<br>for $\text{Si}_3\text{N}_4$ Containing $\text{BeSiN}_2$ and $\text{Y}_2\text{O}_3$ Additives..... | 31          |
| Table IV   | Phases Present as a Function of Temperature<br>for the "Grain Boundary Composition".....   | 32          |
| Table V    | Optimization of the Sintering Process for $\text{Si}_3\text{N}_4$<br>Containing $\text{BeSiN}_2$ and $\text{Y}_2\text{O}_3$ Additives.....                       | 33          |
| Table VI   | Room Temperature MOR for the (2.5, 3) and (3,3)<br>Compositions.....   | 34          |
| Table VII  | Steady State Creep Rates of the (2.5, 3) and (3,3)<br>Compositions.....  | 36          |
| Table VIII | Phases Present as a Function of Composition<br>After GPS at $2050^\circ\text{C}$ .....   | 42          |
| Table IX   | Densification of $\text{Si}_3\text{N}_4$ Containing $\text{LiAl}_5\text{O}_8$ and $\text{YF}_3$<br>Additives.....  | 44          |
| Table X    | Phases Present as a Function of Temperature for $\text{Si}_3\text{N}_4$<br>Containing $\text{LiAl}_5\text{O}_8$ and $\text{YF}_3$ Additives.....                 | 45          |
| Table XI   | Densification of $\text{Si}_3\text{N}_4$ Containing a Variety of Additives.....  | 47          |
| Table XII  | Powder Characterization of the Ube-SN-E10 $\text{Si}_3\text{N}_4$ .....  | 49          |
| Table XIII | Densification of Ube $\text{Si}_3\text{N}_4$ .....   | 50          |

FOREWORD

This development work has been sponsored by the Army Materials and Mechanics Research Center under AMMRC/DOE Interagency Agreement EC-76-A-1017-002 as part of the DOE, Office of Vehicle and Engine R&D, Ceramic Technology for Advanced Heat Engines Program. It has been carried out in the Inorganic Materials Laboratory of General Electric Corporate Research and Development, Schenectady, New York under Contract DAAG46-82-C-0053 during the period September 1982-February 1983. Mr. George Gazza was the program monitor.

The author would like to acknowledge Dr. R. J. Charles for his overall guidance of the program, Dr. C. D. Greskovich for useful discussions, and D. T. Outhouse for his ceramic processing skills. D. G. Polensky is also acknowledged for his contributions to the program.

|                    |                                     |
|--------------------|-------------------------------------|
| Accession For      |                                     |
| NTIS GRA&I         | <input checked="" type="checkbox"/> |
| DTIC TAB           | <input type="checkbox"/>            |
| Unannounced        | <input type="checkbox"/>            |
| Justification      |                                     |
| By                 |                                     |
| Distribution/      |                                     |
| Availability Codes |                                     |
| Dist               | Avail and/or<br>Special             |
| A1                 |                                     |

DTIC COPY INSPECTOR 2

## SUMMARY OF IMPORTANT RESULTS

The sintering of  $\text{Si}_3\text{N}_4$  containing  $\text{BeSiN}_2$  and  $\text{Y}_2\text{O}_3$  was examined and found to yield densities greater than 99% on routine basis. A composition containing 2.5 w/o  $\text{BeSiN}_2$  and 3.0 w/o  $\text{Y}_2\text{O}_3$  displayed a room temperature modulus of rupture of greater than 690 MPa and a fracture toughness  $K_{IC}$  of about  $6 \text{ MNm}^{-3/2}$ , a creep rate of  $4 \times 10^{-5} \text{ h}^{-1}$  at  $1300^\circ\text{C}$  under a 69 MPa load, and a parabolic rate constant for oxidation at  $1350^\circ\text{C}$  of  $1.7 \times 10^{-11} \text{ kg}^2\text{m}^{-4}\text{s}^{-1}$ . The presence of  $\text{Y}_2\text{O}_3$  in conjunction with  $\text{BeSiN}_2$  permitted sintering at lower temperature than the baseline composition which contained 7 w/o  $\text{BeSiN}_2$  and 3.5 w/o oxygen. The lower sintering temperature resulted in a material having a finer grain size and subsequently a higher strength. The increased strength was also influenced by the presence of a significant fraction of elongated grains in the microstructure which has been previously reported to increase both strength and fracture toughness. This composition has adequate properties for structural applications except for the high creep rate, which is on the same order as NC-132.

The sintering of  $\text{Si}_3\text{N}_4$  containing 5 w/o  $\text{LiAl}_5\text{O}_8$  and 3 w/o  $\text{YF}_3$  was examined and found to yield densities greater than 97%. The creep rate of this composition was  $5 \times 10^{-3} \text{ h}^{-1}$  at  $1300^\circ\text{C}$  under a load of 69 Mpa. The high creep rate, in conjunction with a moderately high oxidation rate, precludes the use of this material for high temperature structural applications.

A new  $\text{Si}_3\text{N}_4$  powder from Ube Industries Ltd. was examined and found to sinter to greater than 98.5% using the baseline composition and minimal processing. Although thermomechanical measurements have not been conducted, the Ube powder appears to be a suitable substitute for GTE Sylvania SN502.

Several other possible sintering aids were examined; however, none of them proved to be viable approaches for producing high density, sintered  $\text{Si}_3\text{N}_4$ .

## I. INTRODUCTION

Silicon nitride based materials have received a great deal of attention in the past 10 years for potential applications in small automotive gas turbines, turbochargers and a variety of other high temperature structural applications. The most demanding application would be as a gas turbine rotor where temperatures of approximately 1300°C and stresses up to 690 MPa are anticipated. In order for a material to acceptably perform as a turbine rotor it must have high strength (690 MPa), high Weibull modulus, high fracture toughness, high creep resistance and high oxidation resistance. Over the years several fabrication routes have been developed to produce the complex rotor shape and each route has its own particular advantages and disadvantages. Hot pressed  $\text{Si}_3\text{N}_4$  has proven to yield material with acceptable room temperature properties; however, the presence of a liquid phase densification aid results in degradation of high temperature strength. It is difficult to mass produce into complex shapes in a cost effective fashion since only simple shapes can be hot pressed and subsequent diamond grinding of a monolithic rotor becomes totally out of the question with regard to cost. Although reaction-bonded  $\text{Si}_3\text{N}_4$  can be conveniently mass produced into intricate shapes and exhibits adequate creep properties, it suffers from poor oxidation behavior (because of the high residual porosity of approximately 15%) and low fracture strength (less than 500 MPa). Recently, Ford Motor Company has developed a process whereby they first reaction bond and then sinter the material at high temperature and pressure using  $\text{Y}_2\text{O}_3$  sintering aid. The resultant material is greater than 99% dense and thereby eliminates the problem of severe oxidation associated with material which is only reaction-bonded. However, the strength retention at high temperature, intermediate temperature oxidation resistance, and creep resistance may be affected by the presence of certain yttrium silicon oxynitride compounds. The last approach to the fabrication of  $\text{Si}_3\text{N}_4$  materials has been by sintering. Because of

the inadequacies of reaction-bonded and hot-pressed forms of silicon nitride, the development of sintered  $\text{Si}_3\text{N}_4$  was cited as a priority goal for materials development for small automotive gas turbine engines in 1974<sup>(1)</sup>. In fact, it was in 1974 that developments in  $\text{SiC}$ <sup>(2)</sup> and  $\text{Si}_3\text{N}_4$ <sup>(3)</sup> research led to the fabrication of dense (greater than 90% of theoretical density) ceramics by the sintering process. Since that time a number of liquid phase sintering aids have been investigated, and sintering to greater than 99% density has been reported for several compositions.

There are a number of difficulties in sintering  $\text{Si}_3\text{N}_4$  to full density with good thermomechanical properties.  $\text{Si}_3\text{N}_4$  is a covalently bonded solid (approximately 70% covalency<sup>(4)</sup>) and consequently, a large amount of energy is required for the formation and motion of structural defects which permit diffusion and subsequent sintering. Since densification (macroscopic shrinkage) of powder compacts of  $\text{Si}_3\text{N}_4$  must take place by grain boundary and/or volume diffusion mechanisms, chemical additives and high temperatures are usually required to increase the densification kinetics by increasing the effective diffusion coefficients of the rate-limiting species (generally assumed to be N, based on self-diffusion measurements<sup>(5)</sup>). In addition, submicrometer particle sizes are usually employed to increase the sintering kinetics as well as the rate of chemical reaction between the additive phase(s) and the  $\text{Si}_3\text{N}_4$ .

Typically, the chemical additives selected for  $\text{Si}_3\text{N}_4$  form a liquid phase during sintering by reacting with the  $\text{SiO}_2$  (and impurities) on the  $\text{Si}_3\text{N}_4$  particles. As densification proceeds, the  $\alpha\text{-Si}_3\text{N}_4$  (low temperature polymorph) dissolves in the liquid phase and precipitates out as  $\beta\text{-Si}_3\text{N}_4$ <sup>(6-9)</sup> and sintering proceeds via a solution-reprecipitation process. This  $\text{SiO}_2$ -rich glassy phase resides along the grain boundaries and at triple points and degrades the thermomechanical properties by grain boundary sliding<sup>(10,11)</sup> and intergranular creep cavitation<sup>(11-13)</sup> mechanisms. Improved thermomechanical properties have been achieved by (1) reducing

the amount of residual glassy phase, (2) compositional control and subsequent crystallization of the glassy phase, and (3) increased viscosity of the glassy phase. However, the densification rate of  $\text{Si}_3\text{N}_4$  is generally decreased by reducing the amount of liquid phase or by increasing its viscosity. To counterbalance the limited sinterability, higher temperatures (greater than  $1800^\circ\text{C}$ ) are generally required, which then introduces the problem of thermal decomposition of  $\text{Si}_3\text{N}_4$ <sup>(14)</sup> and the glassy phase, resulting in density regression and a low density final product. Experiments have shown<sup>(15)</sup>, however, that thermal decomposition can be minimized or controlled by using  $\text{N}_2$  pressures of approximately 2 MPa. The development of fully-dense, sintered  $\text{Si}_3\text{N}_4$  depends strongly on the competition between rates of densification and thermal decomposition. This approach requires acceptance of the inconvenience of sintering  $\text{Si}_3\text{N}_4$  at high temperatures and high pressures.

Under two previous contracts with DOE/AMMRC (#DAAG46-78-C-0058<sup>(16)</sup> and #DAAG46-81-C-0029)<sup>(17)</sup>, General Electric has pursued the sintering of  $\text{Si}_3\text{N}_4$  using 7 w/o  $\text{BeSiN}_2$  and 7 w/o  $\text{SiO}_2$  sintering aids. In the first contract, the two-step gas pressure sintering (GPS) process was developed, the composition was optimized, and the thermomechanical properties were determined. In the second contract, the GPS process was further studied and optimized, the process was scaled-up to produce larger test bars and the thermomechanical properties were again determined. Table I presents the properties of the original small test bars and the scaled-up test bars. The Table reports the MOR at room temperature and at high temperature ( $1300\text{-}1500^\circ\text{C}$ ), the creep rate, oxidation rate, fracture toughness and Vicker's hardness. The results show that the material had unexcelled creep and oxidation characteristics relative to any sintered  $\text{Si}_3\text{N}_4$  reported to date. The absolute strength of the material at room temperature was lower than other forms of sintered  $\text{Si}_3\text{N}_4$ ; however, the strength retention was superior. Tests

conducted at AMMRC by G. D. Quinn showed that a stress rupture specimen survived 276 MPa (40,000 psi) leaching for 10,000 h at 1200°C and had a total creep strain of <0.1%. This outstanding result has heretofore not been demonstrated with Si<sub>3</sub>N<sub>4</sub> ceramics. The retained strength of the 10,000 h survivor was 442 MPa, a value higher than the average baseline strength. The high sintering temperature and subsequently the large grain size is believed to be responsible for the lower room temperature MOR.

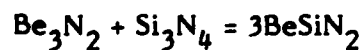
## II. SCOPE OF THE WORK

The general scope of the program has been to find methods to reduce the final β-Si<sub>3</sub>N<sub>4</sub> grain size of the GPS Si<sub>3</sub>N<sub>4</sub> so that fracture strengths at room temperature and at high temperature (approximately 1300°C) may routinely exceed 690 MPa (100,000 psi). Another important aspect of the work has been to reduce or preferably eliminate the BeSiN<sub>2</sub> and still maintain the excellent properties which have been achieved with GPS Si<sub>3</sub>N<sub>4</sub> containing 7 w/o BeSiN<sub>2</sub> and approximately 3.5 w/o oxygen. Once a suitable, non-beryllium containing additive has been identified, fracture strength at room temperature and 1300°C, creep, and oxidation characteristics were to be determined.

## III. EXPERIMENTAL PROCEDURE

### A. Preparation of BeSiN<sub>2</sub>

The sintering aid, BeSiN<sub>2</sub>, was prepared by mixing equimolar quantities of Be<sub>3</sub>N<sub>2</sub> and Si<sub>3</sub>N<sub>4</sub> and reacted according to the reaction:



The reactants were mixed in a Nalgene jar mill for 1 hour using heptane and Si<sub>3</sub>N<sub>4</sub> milling media. After mixing, the slurry was dried in an N<sub>2</sub> glove box for 12 hours, collected and isostatically pressed (approximately 14 MPa) into a slug. The green

slug was placed in a BN crucible and reacted at approximately 1600°C for 20 minutes under 2-3 MPa N<sub>2</sub> pressure. The resulting powder was confirmed by XRD to be BeSiN<sub>2</sub> plus a trace of β-Si<sub>3</sub>N<sub>4</sub>.

#### B. Preparation of Y<sub>2</sub>O<sub>3</sub>

Yttrium oxide was prepared by first forming yttrium oxalate and then calcining in air to yield the oxide. First, 80g of oxalic acid was dissolved in 100 ml of distilled water. In a separate beaker, 100g of Y(NO<sub>3</sub>)<sub>3</sub>·4H<sub>2</sub>O was dissolved in 175 ml of distilled water. The yttrium nitrate solution was added dropwise to the oxalic acid solution which was stirred vigorously with a magnetic stirrer. The yttrium oxalate precipitate was then washed thoroughly with 11 liters of distilled water and finally drawn down on a filter paper in a Buchner funnel. The yttrium oxalate was dried in an oven at 110°C and then calcined at 650°C in air to yield a Y<sub>2</sub>O<sub>3</sub> powder with a specific surface area of approximately 10 m<sup>2</sup>/g.

#### C. Preparation of LiAl<sub>5</sub>O<sub>8</sub>

Reagent grade LiOH and high purity Al<sub>2</sub>O<sub>3</sub> were wet milled in a Nalgene jar with heptane and alumina milling media on a paint shaker for 60 minutes. The batch was reduced to dryness, placed in an alumina crucible and reacted at 1100°C for 2 hours in air. Analysis by XRD showed that LiAl<sub>5</sub>O<sub>8</sub> had formed with a trace of α-Al<sub>2</sub>O<sub>3</sub> present.

#### D. Batch Preparation for Initial Compositional Studies

Sylvania SN502 was selected as the initial powder source based on the large amount of experience that we have with that powder. A batch containing 200g SN502 Si<sub>3</sub>N<sub>4</sub> + 7 w/o addition of BeSiN<sub>2</sub> was ball milled for 72 hours in a steel mill

using heptane as a liquid medium. The milled powder was leached for approximately 12 hours with a solution of 7.4% HCl and 9.1% HNO<sub>3</sub> to remove the metallic impurities introduced during milling. The Si<sub>3</sub>N<sub>4</sub> slurry was then washed repeatedly with distilled water until there was no detection of Fe<sup>2+</sup> ions by the K<sub>3</sub>Fe(CN)<sub>6</sub> test. The next step involved washing the powder with acetone to remove the Cl<sup>-</sup> ions and this was done until there was a negative test using Ag(NO<sub>3</sub>). After the acetone washing was complete, the powder was dried for approximately 12 hours under a heat lamp in a ventilated hood. In addition, there was a batch of Si<sub>3</sub>N<sub>4</sub>, containing no BeSiN<sub>2</sub> additive, prepared in the same fashion described above.

The Si<sub>3</sub>N<sub>4</sub> + 7 w/o BeSiN<sub>2</sub> batch was then mixed in a Nalgene jar with heptane and Si<sub>3</sub>N<sub>4</sub> media on a paint shaker with the milled Si<sub>3</sub>N<sub>4</sub> powder, containing no additive, to yield powders containing 1,2, and 3 w/o BeSiN<sub>2</sub>. The Y<sub>2</sub>O<sub>3</sub> was then added to the three powder batches by wet mixing in a mortar and pestle to obtain 1,2, and 3 w/o addition of Y<sub>2</sub>O<sub>3</sub> to each of the Si<sub>3</sub>N<sub>4</sub> + x BeSiN<sub>2</sub> compositions.

Several other additives were investigated in addition to the BeSiN<sub>2</sub> and Y<sub>2</sub>O<sub>3</sub> additives. Those batches were prepared by mixing the previously milled, leached and washed SN502 Si<sub>3</sub>N<sub>4</sub> powder with the appropriate amount of additive in a Nalgene jar with heptane and Si<sub>3</sub>N<sub>4</sub> media on a paint shaker.

#### E. Batch Preparation for Optimized Compositions

Once the optimum compositions were determined for the sintering of Si<sub>3</sub>N<sub>4</sub> using BeSiN<sub>2</sub> and Y<sub>2</sub>O<sub>3</sub> additives, 100g batches were prepared. The batch, containing Si<sub>3</sub>N<sub>4</sub> and the appropriate amount of additive was wet milled for 72 hours in a steel mill with heptane. The milled powder was acid leached, water washed, acetone washed, and dried as described above. The Y<sub>2</sub>O<sub>3</sub> was then added

by wet mixing in a Nalgene jar with heptane and  $\text{Si}_3\text{N}_4$  balls for 60 minutes on a paint shaker. The batch was finally reduced to dryness and was ready for powder compaction.

#### F. Powder Compaction

Samples (approximately 1g) were first die pressed in a 3/8" diameter double-acting die at 28 MPa followed by cold isostatic pressing at approximately 200 MPa. A lubricant solution consisting of oleic acid, stearic acid and dibutyl phthalate dissolved in 2-propanol was used to aid in pressing. The lubricant solution was mixed with the powder in a mortar and pestle and the propanol was allowed to evaporate before pressing. Mechanical test bars were prepared by the above procedure from green compacts having a weight of approximately 6g and dimensions of approximately 0.8 x 0.8 x 5.8 cm.

### IV. SINTERING AND PROPERTY STUDIES USING $\text{BeSiN}_2$ AND $\text{Y}_2\text{O}_3$ ADDITIVES

#### A. Initial Sintering Studies Using $\text{BeSiN}_2$ and $\text{Y}_2\text{O}_3$ Additives

The sintering behavior of 12 different compositions containing various amounts of  $\text{BeSiN}_2$  and  $\text{Y}_2\text{O}_3$  was investigated using the two-step GPS process. A soak temperature of  $2035^\circ\text{C}$  for 30 minutes under 2 MPa  $\text{N}_2$  pressure was used in the first step and  $1950^\circ\text{C}$  for 30 minutes under 6.9 MPa  $\text{N}_2$  pressure in the second step. Table II presents the composition, the weight loss during sintering ( $\Delta W/W_0$  %), the oxygen content (w/o oxygen) and the fired density (%  $\rho$ ). There are five compositions which yield densities greater than 93% of theoretical and the compositions containing 3 w/o  $\text{BeSiN}_2$  and 1,2, and 3 w/o  $\text{Y}_2\text{O}_3$  all achieved nearly full density. It should be noted that the oxygen content of all compositions was less than the approximately 3.2 w/o oxygen required to densify the baseline composition which contains 7 w/o  $\text{BeSiN}_2$ . The oxygen contents reported in Table II include the oxygen associated with the  $\text{Y}_2\text{O}_3$  and the maximum value was 2.5

w/o. Based on the initial investigation using  $\text{BeSiN}_2$  in conjunction with  $\text{Y}_2\text{O}_3$  sintering aid, it became apparent that the high temperature phase equilibria of the liquid phase was strongly effected by the  $\text{Y}_2\text{O}_3$  addition.

The densification behavior as a function of temperature was examined for six compositions which contained 1.5, 2.0, and 3.0 w/o  $\text{BeSiN}_2$  in conjunction with 2.0 and 3.0 w/o  $\text{Y}_2\text{O}_3$  for each of the 3 levels of  $\text{BeSiN}_2$ . Each of the six compositions was fired at 1600, 1700, 1800, 1875, 1950, 2030, and 2100°C for 20 minutes with a 2 MPa  $\text{N}_2$  overpressure. Weight loss and density measurements were made on each sample after firing. An abbreviated notation will be used throughout the report which will list the % of  $\text{BeSiN}_2$  first and the %  $\text{Y}_2\text{O}_3$  second. For example, a composition containing 1.5 w/o  $\text{BeSiN}_2$  and 2 w/o  $\text{Y}_2\text{O}_3$  will be denoted as a (1.5,2) composition. Figure 1 presents the densification behavior as a function of temperature for the (1.5,2), (2,2), and the (3,2) compositions. Densification was observed to begin above 1700°C for the (2,2) and the (3,2) compositions and above 1800°C for the (1.5,2) composition. The (1.5,2) composition reached a maximum density of 80.2% at 2100°C which is clearly not a viable composition since closed porosity (approximately 92%) was not achieved. The (2,2) composition reached a maximum density of 90.1% at 2030°C. The decrease in density at the higher temperature is similar to the observations made for the baseline composition which contained 7%  $\text{BeSiN}_2$  and 3.5% oxygen<sup>(16)</sup>. The (3,2) composition, however, displayed increasing density with increasing temperature up to a maximum of 96.6% at 2100°C. Figure 2 presents the densification behavior as a function of temperature for the (1.5,3), (2,3), and the (3,3) compositions. The curves are generally of the shape as those shown in Figure 1. The (3,3) composition, however, reached a density of 99.4% at 2100°C. A point to be noted was the fact that the compositions containing  $\text{BeSiN}_2$  and  $\text{Y}_2\text{O}_3$  could be sintered to greater than 93% in a single step firing cycle. This is in contrast to the baseline composition which required the 2-step GPS process.

Another significant result of this sintering study is shown in Table III, which presents the weight change during sintering as a function of temperature for the six compositions. It was observed that the specimens first experience a weight gain followed by a weight loss at higher temperature. However, the compositions that showed the highest density also showed essentially no net weight loss, as in the case of the (3,2) composition, and a net weight gain for the (3,3) composition which achieved densities of 96.6% and 99.4%, respectively. This observation is in contrast to the behavior of the baseline composition which always displayed a net weight loss of greater than 1%. The weight loss of the baseline composition was attributed to the loss of  $\text{SiO}_{(g)}$  as the composition of the liquid phase moved toward equilibrium. The loss of oxygen was confirmed by neutron activation analysis<sup>(17)</sup>. The weight gain of the  $\text{BeSiN}_2\text{-Y}_2\text{O}_3$  containing compositions may possibly be due to  $\text{N}_2$  dissolution into the liquid phase as equilibrium is approached. The subsequent weight loss at high temperature may be attributed to the loss of  $\text{SiO}_{(g)}$  or  $\text{N}_2$  as the higher temperature equilibrium is achieved.

#### B. "Grain Boundary Composition" Study

An observation was made that although the outside of sintered samples appeared to be fully dense, the interior had a slightly lower density as indicated by the lighter color. It was speculated that gas generating reactions were occurring during sintering and insufficient time was being allowed to permit the gases to escape prior to pore closure. Several attempts at changing the heating schedule during sintering to allow the gases to escape before the porosity closed off were shown to help, but the problem was not totally eliminated. In order to further understand the origin of the gas generating reactions, which are at least partially responsible for the lower density regions in the samples, a study of the phase relations versus temperature was initiated. The approach was to try to simulate the development of the grain boundary phase which is responsible for densification. The composition that was chosen corresponded to the sintering of  $\text{Si}_3\text{N}_4$  containing

3 w/o  $\text{BeSiN}_2$  and 3 w/o  $\text{Y}_2\text{O}_3$ . The oxygen content of the  $\text{Si}_3\text{N}_4$  powder was measured by neutron activation analysis to be 1.86 w/o which corresponds to approximately 3.5 w/o  $\text{SiO}_2$ . The "grain boundary composition" was prepared by wet mixing 3.0g  $\text{BeSiN}_2$ , 3.0g  $\text{Y}_2\text{O}_3$ , and 3.5g  $\text{SiO}_2$  in a Nalgene jar with heptane and  $\text{Si}_3\text{N}_4$  media on a paint shaker for 30 minutes. The batch was dried, die pressed into pills at 126 MPa and reacted at temperatures of 1400, 1500, 1600, 1700, 1900, and 2050°C for 30 minutes under 2 MPa  $\text{N}_2$  pressure. After reaction, the samples were ground and the phases were determined by XRD. Table IV presents the phases that existed as a function of temperature. The phases present may, in fact, not represent the equilibrium phases, particularly at the lower temperatures, since only a 30 minute hold at each temperature was allowed. At 1400°C, the phases present were  $\text{BeSiN}_2$ ,  $\text{Si}_2\text{N}_2\text{O}$ ,  $\text{Y}_2\text{Si}_2\text{O}_7$ ,  $\text{Be}_2\text{Y}_2\text{SiO}_7$ , and some liquid. At 1500°C, the number of phases had decreased and the phases present were  $\text{Be}_2\text{Y}_2\text{SiO}_7$ ,  $\text{Si}_2\text{N}_2\text{O}$ , and liquid. Microscopic examination of the reacted samples revealed that only a small amount of liquid phase had formed at 1400 and 1500°C. At 1600°C, a significant amount of liquid phase had formed and there was considerable amounts of gas generated as evidenced by severe bloating of the sample. The phases present were  $\beta\text{-Si}_3\text{N}_4$ ,  $\text{Be}_2\text{Y}_2\text{SiO}_7$ ,  $\text{Y}_2\text{Si}_2\text{O}_7$ , and liquid. The same severe bloating was observed at 1700°C and the phases present were  $\beta\text{-Si}_3\text{N}_4$ , liquid, and a trace of  $\text{Be}_2\text{Y}_2\text{SiO}_7$  and  $\text{Y}_2\text{Si}_2\text{O}_7$ . At 1900°C the entire sample had melted and formed a liquid that had very few gas bubbles remaining in the solidified melt and the only remaining crystalline phase was  $\beta\text{-Si}_3\text{N}_4$ . The X-ray pattern showed broadening of the peaks and for this reason it is believed that the  $\beta\text{-Si}_3\text{N}_4$  precipitated out during cooling. After reaction at 2050°C, the only crystalline phase was  $\beta\text{-Si}_3\text{N}_4$  and there were essentially no gas bubbles trapped in the solidified melt, thus indicating that no significant gas evolving reactions were occurring. Previous sintering studies have shown that the porosity closes off at approximately 92% density, which occurs at about 2000°C as shown in Figure 2. The "grain boundary" study showed that the reactions giving rise to gas generation were complete by

1900°C, while the porosity was still open, and therefore the low density centers of the samples were affected by something in addition to gas generation.

### C. Optimization of the Sintering Process

The results from the "grain boundary" study indicated that it would be beneficial to have a slow heating schedule in the temperature range of 1700 to 1900°C to allow for gas evolution prior to pore closure. Table V presents the results of the sintering experiments directed toward optimization of the sintering process. Samples 1-3 were fired in a BN crucible with a modified heating schedule and the samples achieved relatively high density (theoretical density for the (2.5,3) composition is 3.23 g/cc). However, microscopic examination revealed that the problem of the lower density interior of the sample was not completely eliminated. The use of a reaction-bonded  $\text{Si}_3\text{N}_4$  (RBSN) crucible essentially eliminated the density gradient. It has been previously reported that BN crucibles have an adverse affect on sintering and it is no surprise that the RBSN crucible gave better results. The optimized sintering schedule involved the use of an RBSN crucible and a heating schedule that requires at least a 30 minutes duration for heating from 1700 to 1900°C. The furnace was then rapidly heated to 2025°C for a 30 minute hold under 2 MPa  $\text{N}_2$  pressure followed by a 30 minute hold a 1950°C under 6.9 MPa  $\text{N}_2$  pressure. The optimized sintering process resulted in densities of greater than 99% for the (2.5,2.5), (2.5,3), and the (3,3) compositions.

### D. Properties of $\text{Si}_3\text{N}_4$ Containing $\text{BeSiN}_2$ and $\text{Y}_2\text{O}_3$ Additives

#### D.1. Room Temperature Modulus of Rupture

The (2.5,3) and the (3,3) compositions were selected for scale-up to produce test bars for mechanical property measurements. Six test bars of each composition were prepared using the 2-step GPS process. Modulus of rupture measurements were conducted to compare the strength of the (2.5,3) and the (3,3) compositions with the baseline composition which contained 7%  $\text{BeSiN}_2$  and 7%  $\text{SiO}_2$  sintering

aids. Three-point bend specimens were prepared by surface grinding the samples with a 320 grit wheel at 0.0005" per pass until the faces were flat and parallel. Then 0.0002" was removed from each face with a 500 grit wheel at 0.0002" per pass. Finally, the edges were hand chamfered with a 15  $\mu$ m diamond lap. The modulus of rupture was determined by 3-point bend with a span of 3.8 cm and a crosshead speed of 0.5 mm/min and the results are presented in Table VI.

The (2.5,3) composition displayed excellent room temperature strength with the average MOR being 691 MPa (100,202 psi). It should be noted that 5 of the bars had strength greater than 690 MPa and one bar failed at 490 MPa. Microscopic examination revealed that a severe machining flaw was present in the low strength bar. If this bar is dropped from the data, the average strength was 731 MPa. The (3,3) composition had an average strength of 542 MPa. The strength of the (3,3) composition was lower than the (2.5,3) composition, however, it was higher than the average strength of the baseline composition with was 440 MPa.

#### D.2. Examination of Fracture Surfaces

Examination of the fracture surfaces of the (2.5,3) and the (3,3) compositions by scanning electron microscopy revealed a great deal of information regarding the increase in MOR relative to the baseline composition. The fracture surfaces of the 3 compositions are shown in Figure 3 a,b, and c. The most notable and obvious change was that the baseline composition fractured by a transgranular mode whereas the  $\text{BeSiN}_2\text{-Y}_2\text{O}_3$  containing specimens failed by a mode that appears to be a mixture of transgranular and intergranular fracture. Examination of the microstructures revealed that the grain sizes of both the (2.5,3) and the (3,3) - compositions were smaller than the grain size of the baseline composition. This observation was to be expected since the baseline composition was sintered at 2100°C compared to 2025 C for (2.5,3) and the (3,3) samples. It is well known that

the smaller the grain size, the greater the room temperature strength of the material. It was previously noted<sup>(17)</sup> that final grain size of sintered  $\text{Si}_3\text{N}_4$  is quite sensitive to both temperature and time at temperature. The sintering of  $\text{Si}_3\text{N}_4$  containing  $\text{BeSiN}_2\text{-Y}_2\text{O}_3$  additions was observed to display the same sensitivity of grain size as a function of temperature and sintering studies were conducted to determine the minimum temperature required to achieve full density and thus, maximize strength. Another significant difference between the (2.5,3) and (3,3) compositions and the baseline composition was the appearance of elongated grains which take on both an acicular and a platelet morphology. It appears that fracture occurs primarily by an intergranular mode as the fracture front passes through a region of fine and acicular grains. However, the large platelets appear to fracture transgranularly. The presence of elongated grains has been reported to increase the room temperature strength and fracture toughness and their appearance is generally associated with presence of  $\text{Y}_2\text{O}_3$  or  $\text{MgO}$  in the liquid phase. The presence of the elongated grains and the smaller grain size is probably the cause of increased room temperature strength for the (2.5,3) and (3,3) compositions relative to the baseline composition. The reason is not at all clear why the (2.5,3) specimens showed significantly higher strength than the (3,3) specimens. The grain size of the (2.5,3) appears to be slightly smaller than the (3,3), however, the difference in grain size alone shouldn't account for the large difference in strength.

### D.3. Creep

The creep behavior of the (2.5,3) and (3,3) compositions were measured in air at a constant stress of 69 MPa and temperatures of 1200, 1300 and 1350°C. The creep specimens (0.25 x 0.25 x 4.5 cm) were loaded in a 3-point bending mode using SiC fixtures with a test span of 2.24 cm. Deflection of the test specimen was measured with a DC-operated LVDT which had a sensitivity of 80 volts/cm. The

furnace was heated from room temperature to the test temperature over a 6 hour period and allowed to equilibrate overnight before applying the stress of 69 Mpa which was accomplished by dead weight loading external to the furnace. Table VII presents the calculated steady state creep rates for various compositions and temperatures. The (2.5,3) specimen displayed a steady state creep rate of  $4.2 \times 10^{-5} \text{ h}^{-1}$  at  $1300^{\circ}\text{C}$  compared to  $4.6 \times 10^{-7} \text{ h}^{-1}$  for the baseline composition under identical conditions. This two order of magnitude increase in creep rate was not anticipated. It has been reported by other workers that the creep rate of  $\text{Si}_3\text{N}_4$ , which was densified in the presence of a liquid phase, can be decreased by a heat treatment which causes crystallization of the residual glassy phase present at the grain boundaries and triple points. A (2.5,3) specimen was heat treated at  $1650^{\circ}\text{C}$  for 3 hours under 6.9 MPa  $\text{N}_2$  pressure in an attempt to cause crystallization of the residual glassy phase. XRD analysis after heat treatment revealed that the  $\text{Be}_2\text{Y}_2\text{SiO}_7$  and  $\text{Y}_2\text{Si}_2\text{O}_7$  minor phases that were present before heat treatment were still present but the amount of those phases was increased at the surfaces of the specimen. Table VII shows that the heat treated sample, designated as (2.5,3)HT, displayed essentially no reduction in creep rate due to heat treatment. It would appear that the decrease in creep rate due to heat treatment occurs only for specific compositions and no gain was achieved with the (2.5,3) composition. The (3,3) composition showed a slightly higher creep rate and was not surprising due to the increased amount of additive. Although, both the (2.5,3) and (3,3) compositions show the crystallized phases  $\text{Be}_2\text{Y}_2\text{SiO}_7$  and  $\text{Y}_2\text{Si}_2\text{O}_7$  to be present at room temperature, they apparently react at higher temperature to yield a low melting, low viscosity liquid and cause a subsequent degradation in high temperature strength characteristics. The strength degradation was so severe that neither composition could maintain a 69 MPa load at  $1400^{\circ}\text{C}$ .

#### D.4. Oxidation

The oxidation behavior of the (2.5,3) and the (3,3) compositions was examined at 1300 and 1350°C in Al<sub>2</sub>O<sub>3</sub> tube furnace with flowing oxygen for times up to 261 hours. Oxidation experiments were conducted on clean test pieces which were finished with 500 grit diamond and leached for 2 hours in concentrated HCl followed by washing in distilled water and alcohol. The specimens were placed on an oxidized SiC setter which lay on an Al<sub>2</sub>O<sub>3</sub> boat and inserted into the hot furnace within 5 minutes. During the oxidation experiment, the furnace was controlled within +/- 2°C. The specimens were periodically removed from the hot furnace and its weight measured on a Mettler H54 AR balance capable of measuring to the nearest 2 x 10<sup>-5</sup> g. The amount of oxidation was determined from the weight gain measurements. Parabolic oxidation kinetics were observed and the parabolic rate constant (k<sub>p</sub>) was determined using the equation:

$$(\Delta W/A)^2 = k_p t$$

where  $\Delta W/A$  was the change in weight per unit area and  $t$  is the oxidation time.

Figure 4 presents the oxidation behavior of the (2.5,3), (3,3) and the baseline composition at 1300°C and the parabolic rate constants were calculated to be 5.7 x 10<sup>-12</sup>, 2.8 x 10<sup>-11</sup>, and 7.4 x 10<sup>-13</sup> kg<sup>2</sup>m<sup>-4</sup>s<sup>-1</sup> respectively. Figure 5 presents the oxidation behavior at 1350°C of the same three compositions and a Y<sub>2</sub>O<sub>3</sub>-Al<sub>2</sub>O<sub>3</sub> composition prepared by GTE Sylvania. The parabolic rate constants, k<sub>p</sub>, for the (2.5,3), (3,3) and the baseline compositions were 1.7 x 10<sup>-11</sup>, 2.7 x 10<sup>-11</sup>, and 1.4 x 10<sup>-12</sup> kg<sup>2</sup>m<sup>-4</sup>s<sup>-1</sup> respectively. It should be noted that the oxidation rates of the samples containing BeSiN<sub>2</sub> and Y<sub>2</sub>O<sub>3</sub> are considerably lower than the compositions containing Y<sub>2</sub>O<sub>3</sub>-Al<sub>2</sub>O<sub>3</sub> additions.

The surfaces of (2.5,3) and (3,3) samples which were oxidized at 1350°C were examined by SEM and the observations are shown in Figure 6 a and b, respectively. Both samples show the presence of 2 crystallized phases having different morphol-

ogy, one needle-shaped and the other more equiaxed. XRD analysis of the oxidized surface revealed the presence of  $Y_2Si_2O_7$  and  $Y_{20}Si_{18}N_4O_{12}$  in addition to  $\beta$ - $Si_3N_4$  and a very large  $\alpha$ -cristobalite peak. XAFS revealed that both crystalline phases contained Si and Y and the regions where the crystallized phase was absent contained only Si. The presence of Be could not be determined by this technique. It was not possible to determine which phase had the needle-like morphology and which phase had the more equiaxed morphology. The point to be noted is that at temperatures of  $1350^\circ C$  the yttrium is mobile enough to diffuse toward the  $SiO_2$  surface layer produced by oxidation and precipitate out as a stable crystalline phase. The same observations have been made in systems using MgO as a sintering aid<sup>(18)</sup>.

#### D.5. Vicker's Hardness and $K_{IC}$ Measurements

The hardness and the fracture toughness,  $K_{IC}$ , were determined by the microhardness indentation technique<sup>(19)</sup> in a Vicker's test using flat, polished samples. The application of a 500g load resulted in sharp indenter impressions with single extension cracks radiating outward from the impression corners. The Vicker's hardness number (VHN) for the (2.5,3) and (3,3) compositions were determined to be 1600 and 1700, respectively. The corresponding values of  $K_{IC}$  were found to be 6.0 for the (2.5,3) composition and 5.9 for the (3,3). The values of  $K_{IC}$  were calculated using the expression:

$$\left( \frac{K_{IC} \phi}{Ha^{1/2}} \right) \left( \frac{H}{E \phi} \right)^{0.4} = 0.142 (c/a)^{-1.56}$$

#### E. Microstructural and Phase Characterization

Several compositions containing the  $BeSiN_2-Y_2O_3$  additive ( (2,2), (2.5,2.5), (2.5,3), (3,3), (3,4), (4,3) ) were examined by scanning electron microscopy and X-ray diffraction to determine the microstructural and phase characteristics.

Figures 7 a and b present the fracture surfaces of the (2.5,3) and (3,3) compositions fired using the 2-step GPS process with a maximum temperature of 2025°C. In comparison, Figures 7 c and d present the fracture surfaces of the same compositions fired using the GPS process with 2050°C being the maximum temperature. It is apparent that the grain size of both compositions increased significantly with only a 25°C increase in sintering temperature. It was noted that the grain size of both the smaller, equiaxed grains as well as the elongated grains increased with increasing temperature. It was shown<sup>(17)</sup> with the baseline composition, which contained 7% BeSiN<sub>2</sub>-7% SiO<sub>2</sub>, that the final grain size of the sintered Si<sub>3</sub>N<sub>4</sub> was strongly affected by the temperature and time at temperature during sintering. From the standpoint of maximizing the room temperature MOR, it is essential that the sintering be done at as low a temperature as possible. Figures 8 a-d presents the fracture surfaces of the (2,2), (2.5,2.5), (3,4) and (4,3) compositions which were fired by the 2-step GPS process with a maximum temperature of 2050°C. The fired density of these compositions was 94.7%, 99.6%, 98.4%, and 97.8%, respectively.

X-ray diffraction of the six compositions led to some very interesting results and are presented in Table VIII. The Table presents the compositions and the phases present after sintering. It was observed that, for the (2,2), (2.5,2.5), (2.5,3), and (3,3) compositions, the major phase was  $\beta$ -Si<sub>3</sub>N<sub>4</sub> and the minor phases were Be<sub>2</sub>Y<sub>2</sub>SiO<sub>7</sub> and Y<sub>2</sub>Si<sub>2</sub>O<sub>7</sub>. However, the (3,4) and (4,3) compositions showed  $\beta$ -Si<sub>3</sub>N<sub>4</sub> as the major phase and only Y<sub>2</sub>Si<sub>2</sub>O<sub>7</sub> as the minor phase. The presence of the Y<sub>2</sub>Si<sub>2</sub>O<sub>7</sub> was expected since the solubility of Y<sub>2</sub>O<sub>3</sub> in  $\beta$ -Si<sub>3</sub>N<sub>4</sub> should be low due to the large atomic radii of yttrium. However, the presence of Be<sub>2</sub>Y<sub>2</sub>SiO<sub>7</sub> was not anticipated based on the previous experience with the baseline composition in which no beryllium-containing second phase was present after sintering. The work of Huseby et al<sup>(20)</sup> showed that there is an appreciable solubility of Be in  $\beta$ -Si<sub>3</sub>N<sub>4</sub>.

Figure 9 presents their findings as a plot of equivalent % Be in  $\beta$ - $\text{Si}_3\text{N}_4$  as a function of temperature. The dotted portion of the curve represents an assumed extrapolation and is not based on any experimental data. It is believed to be a reasonable approximation, however, since the baseline composition contained 2.4 equivalent % Be and firing at  $1950^\circ\text{C}$  in the second step of the GPS process resulted in no Be-containing second phase. Furthermore, lattice fringe imaging in the TEM indicated that if a liquid phase was present at the grain boundary of the baseline composition, it was on the order of  $10 \text{ \AA}$  thick. Based on these results, it was anticipated that the beryllium would dissolve into the  $\beta$ - $\text{Si}_3\text{N}_4$  lattice, thus leaving only an yttrium silicate at the grain boundaries and triple points. It appears that the  $\text{Be}_2\text{Y}_2\text{SiO}_7$  phase is more thermodynamically stable than the solid solution that is formed when beryllium and oxygen dissolve in  $\beta$ - $\text{Si}_3\text{N}_4$ . With respect to the high creep rates of the (2.5,3) and (3,3) compositions, it would appear that a low melting liquid results when  $\text{Be}_2\text{Y}_2\text{SiO}_7$  and  $\text{Y}_2\text{Si}_2\text{O}_7$  are in equilibrium. If this speculation is correct, then one would expect that the creep rates of the (3,4) and (4,3) compositions would be lower than for the (2.5,3) and (3,3) compositions. These tests, however, were not conducted.

## V. Sintering and Properties of $\text{Si}_3\text{N}_4$ Containing $\text{LiAl}_5\text{O}_8$ and $\text{YF}_3$ Additions

### A. Sintering Studies

Sintering experiments were conducted using Ube  $\text{Si}_3\text{N}_4$  and  $\text{LiAl}_5\text{O}_8$  and  $\text{YF}_3$  sintering aids. Table IX presents the additives used, the sintering conditions, the total oxygen content ( $\text{O}_t$ ), the fired density (P) and the weight loss during sintering ( $\Delta\text{W}/\text{W}_0$ ). Table IX shows that the addition of 5%  $\text{LiAl}_5\text{O}_8$  to  $\text{Si}_3\text{N}_4$  resulted in a density of 83% at  $1660^\circ\text{C}$  and that increasing the temperature to  $1920^\circ\text{C}$  gave only a marginal increase in density up to 88%. It was also observed that increasing the oxygen content from 3.9% to as high as 7.9% did not improve the sinterability. The

addition of 3%  $\text{YF}_3$ , however, in conjunction with 5%  $\text{LiAl}_5\text{O}_8$  resulted in densities greater than 96% at temperatures of 1800°C or higher. It should be noted that the addition of  $\text{YF}_3$  resulted in an increased weight loss. The additional weight loss may be attributed to a reaction between  $\text{YF}_3$  and either  $\text{LiAl}_5\text{O}_8$  or  $\text{SiO}_2$  to form  $\text{Y}_2\text{O}_3$  and a volatile specie such as  $\text{SiF}_4$ ,  $\text{AlF}_3$ , or  $\text{LiF}$ . The addition of 10%  $\text{LiAl}_5\text{O}_8$  resulted in similar, but still, inadequate densification. Again, increasing the oxygen content provided no benefit in terms of sinterability.

The compositions containing 5%  $\text{LiAl}_5\text{O}_8$  and 5%  $\text{LiAl}_5\text{O}_8$ -3%  $\text{YF}_3$  were sintered at temperatures ranging from 1700 to 1900°C and XRD was done to determine the phases present. Table X presents a summary of the phases present as a function of temperature for the 2 compositions. It was observed that the compositions containing only  $\text{LiAl}_5\text{O}_8$  retained  $\alpha\text{-Si}_3\text{N}_4$  up to 1900°C whereas the presence of  $\text{YF}_3$  lowered the temperature at which conversion from alpha to beta was complete at less than 1800°C. It appears that the  $\text{LiAl}_5\text{O}_8$  tends to stabilize the alpha phase whereas the presence of  $\text{YF}_3$  tends to enhance the conversion to beta.

## B. Properties

A test bar (0.8 x 0.8 x 5.8 cm before firing) was prepared using Ube  $\text{Si}_3\text{N}_4$  with 5%  $\text{LiAl}_5\text{O}_8$  - 3%  $\text{YF}_3$  composition. The bar was sintered at 1800°C for 2 hours under 1.8 MPa  $\text{N}_2$  pressure and achieved a density of 96%. The fired bar was machined to provide a MOR bar (0.7 x 0.14 x 4.8 cm) and 2 creep specimens (0.25 x 0.25 x 4.8 cm). The MOR bar was broken in 3-point bending mode with a span of 3.8 cm and had a room temperature strength of 466 MPa. Figure 10 is an SEM micrograph of the fracture surface showing the the specimen failed by intergranular fracture. The microstructure appears to be composed of a matrix of 1-2  $\mu\text{m}$  equiaxed grains and a significant fraction of acicular grains.

The creep rate of this composition was determined to be  $5.02 \times 10^{-3}$  at  $1300^{\circ}\text{C}$  under a 69 MPa load. The creep rate was approximately an order of magnitude higher than that measured for NC-132 under the same conditions. This finding is no surprise in light of the fact that sintering to high density could be achieved at  $1800^{\circ}\text{C}$ . The presence of a low melting liquid at the grain boundary is probably the cause of the high creep rate.

The oxidation rate of this material was measured at  $1300^{\circ}\text{C}$  in flowing oxygen. The parabolic rate constant for oxidation at  $1300^{\circ}\text{C}$  was determined to be  $6.76 \times 10^{-11} \text{ kg}^2\text{m}^{-4}\text{s}^{-1}$ . The high rates of creep and oxidation preclude the use of this composition as a high temperature structural material.

#### VI. Evaluation of Various Sintering Aids

Several sintering aids were evaluated in a cursory fashion to determine their effectiveness as a densification aid for  $\text{Si}_3\text{N}_4$ . Table XI presents a summary of these additives, the sintering conditions, the total oxygen content ( $\text{O}_t$ ), the fired density ( $\rho$ ), and the percent weight loss ( $\Delta W/W_0$ ). The addition of either  $\text{Li}_2\text{SiN}_2$  or  $\text{Ga}_2\text{O}_3$  showed virtually no effect on sintering and the addition of  $\text{B}_4\text{C}$  and C resulted in decomposition of the sample. The addition of 10%  $\text{ZrO}_2$  increased the density to 70% as did the addition of 6.8%  $\text{LiAlSiO}_4$ . A slightly higher density of 76% was observed for the addition of 5-10%  $\text{LiAlO}_2$ . The addition of 5%  $\text{LiAlO}_2$  in conjunction with 3%  $\text{YF}_3$  yield a density of 93%. Densities of approximately 80% were realized for additions of 6%  $\text{Y}_2\text{O}_3$  and 5.7%  $\text{Y}_2\text{O}_3$ - 11.7%  $\text{SiO}_2$ . The addition of 10% YAG resulted in densities as high as 95%, a result previously reported by Gazza<sup>(21)</sup>. None of these compositions presented in Table XI were pursued in an attempt to optimize additive content or sintering schedule.

#### VII. Evaluation of Ube $\text{Si}_3\text{N}_4$ Powder

Two different lots of  $\text{Si}_3\text{N}_4$  powder were obtained from Ube Industries on an experimental and trial basis as an alternative to GTE SN502 powder. The Ube powder was produced by first reacting  $\text{SiCl}_4$  with liquid ammonia to form either silicon amide or imide which was subsequently thermally decomposed in the presence of  $\text{N}_2$  or  $\text{NH}_3$  to form  $\text{Si}_3\text{N}_4$ <sup>(22)</sup>. The resultant powder particles have an equiaxed morphology and the presence of very few whiskers as shown in Figure 11a. This is contrary to the powders produced by Sylvania (SN502) which contains a large fraction of whiskers and larger particles as shown in Figure 11b. Note the Figure 11a is magnified 4 times greater than Figure 11b. The SN502 must be extensively milled to break down the whiskers and allow pressing of compacts to a reasonably high green density (approximately 53%). The Ube powder, on the other hand, presses to approximately 53% green density in the as-received state. Because of the powder morphology, it was found that minimal milling was required to produce sintered samples with densities greater than 98%. The sintering aid for all of the experiments was  $\text{BeSiN}_2$ . Table XII presents the chemical and physical properties of the 2 lots of powder as determined by Ube Industries.

Table XIII summarizes the pertinent parameters from the sintering experiments conducted on Lots A-10 and A-18. The oxygen content is listed for each composition, since it was previously established, with SN502 powder, that the oxygen content should be greater than 3.2%. The initial oxygen content was taken from Table XII as reported by Ube, and the oxygen was subsequently adjusted by heating the green compact in air at approximately 1000°C. Specimens were sintered using the two step gas pressure sintering process (GPS) and the sintering conditions are listed in Table XIII according to the Temperature C/ time (minutes) /pressure (MPa) for both the first and second steps. The percent of theoretical density (%P) is based on 3.18 g/cc and the weight loss during sintering is listed as  $W/W_0$ . Specimens were fired in either BN or RBSN crucibles. The column labeled

"Processing" denotes the powder lot and the preparation procedure for producing the green compacts. They are as follows:

- (1) Lot A-10 A 50g batch was prepared by wet mixing  $\text{Si}_3\text{N}_4 + 7$  w/o  $\text{BeSiN}_2$  in a nalgene jar with heptane and  $\text{Si}_3\text{N}_4$  media for 60 minutes on a paint shaker. Pills were cold pressed at 9000 psi and isostatically pressed at 30,000 psi.
- (2) Lot A-10 A 50g batch was prepared by milling  $\text{Si}_3\text{N}_4 + 7$ ; w/o  $\text{BeSiN}_2$  in a steel mill with heptane for 24 hours. The milled batch was leached to remove metallic impurities introduced during milling. Pills were cold pressed at 9000 psi and isostatically pressed at 30,000 psi.
- (3) Lot A-18 Same procedure as (2).

The experiments revealed that the Ube  $\text{Si}_3\text{N}_4$  powder containing 7%  $\text{BeSiN}_2$  and 7%  $\text{SiO}_2$  sintering aids could be repeatedly densified to greater than 98.5% of theoretical. High density could be achieved with a minimum of processing, relative to SN502. It was observed that Lot A-18 gave better microstructural appearance than Lot A-10, which showed a speckled appearance on metallographic sections after sintering. The "speckles" are believed to be due to the presence of approximately 200 ppm Ca in the starting powder. Lot A-18 contained less than 50 ppm Ca and this problem was not apparent for samples prepared from this lot. In general, the same oxygen content and sintering conditions are required to fully densify the Ube powder as was required for SN502. Although thermomechanical property measurements have not been made on specimens prepared from Ube powder, it would appear that, for purposes of this study, UBE powder is an acceptable substitute for SN502.

### VIII. CONCLUSIONS

The sintering of  $\text{Si}_3\text{N}_4$  containing  $\text{BeSiN}_2$  and  $\text{Y}_2\text{O}_3$  additives was examined and found to yield densities greater than 99% of theoretical. The room tempera-

ture strength of the (2.5,3) composition is greater than 690 MPa. The creep resistance of this material, however, is found to be too high to be acceptable as a structural material above 1000°C. Although, the use of BeSiN<sub>2</sub> as a sintering additive requires special handling procedures to deal with possible toxicological issues, it appears to be the best additive yet identified in terms of high temperature strength retention and creep and oxidation resistance. The use of Y<sub>2</sub>O<sub>3</sub> in conjunction with BeSiN<sub>2</sub> served to reduce grain size by decreasing the sintering temperature and subsequently increased the room temperature strength relative to compositions containing 7% BeSiN<sub>2</sub> and 3.5% oxygen. The high temperature strength, however, was substantially degraded and is speculated to be due to the presence of a low melting liquid which occurs when Be<sub>2</sub>Y<sub>2</sub>SiO<sub>7</sub> and Y<sub>2</sub>Si<sub>2</sub>O<sub>7</sub> are in equilibrium.

It is concluded that the use of 7% BeSiN<sub>2</sub> and 3.5% oxygen is an optimum composition in terms of maximizing high temperature properties. It has been shown<sup>(20)</sup> that the solubility of beryllium in β-Si<sub>3</sub>N<sub>4</sub> decreases with increasing temperature. The 2-step GPS process uses this fact by firing at 2100°C in the first step to maximize the amount of liquid present to aid in densification and then dropping the temperature in the second step to 1950°C to permit dissolution of the Be and O in the liquid phase into the β-Si<sub>3</sub>N<sub>4</sub> lattice, thereby effectively drying up the liquid phase. Other systems, particularly the Y<sub>2</sub>O<sub>3</sub>-Al<sub>2</sub>O<sub>3</sub> and Y<sub>2</sub>O<sub>3</sub>-SiO<sub>2</sub>, which utilize a post-sintering heat treatment to crystallize the liquid phase, have shown promise in terms of reducing the creep rate. The presence of a crystallized second phase may result in a strength degradation due to the thermal expansion mismatch between Si<sub>3</sub>N<sub>4</sub> and the second phase during thermal cycling of the gas turbine engine.

## REFERENCES

1. A.E. Gorum, J.J. Burke, E.M. Lenoë, and R.N. Katz, in Proceedings of the NATO-CCMS Symposium on Low Pollution Power Systems Development, Dusseldorf, November 1974.
2. S. Prochazka, in Ceramics for High Performance Applications, edit, by J.J. Burke, A.E. Gorum and R.N. Katz, Brook Hill Pub. Co., Chestnut Hill, MA, 1974.
3. G.E. Terwilliger, *J. Am. Ceram. Soc.* 57, 48 (1974).
4. L. Pauling, The Nature of the Chemical Bond, Cornell Univ. Press. 1939.
5. K. Kijima and S. Shirasaki, "Nitrogen Self-Diffusion in  $\text{Si}_3\text{N}_4$ ", *J. Chem. Phys.* 65 (7) 2668-71 (1976).
6. S. Wild, P. Grieveson K.H. Jack and M.J. Latimer; pp. 377-84 in Special Ceramics 5. Edited by P. Popper. British Ceramic Research Association, Stoke-on-Trent, 1972.
7. R.R. Wills, "Silicon Yttrium Oxynitrides", *J. Am. Ceram. Soc.* 57 (10) 459 (1974).
8. L.J. Bowen, R.J. Weston, T.G. Carruthers and R.J. Brook, "Hot Pressing and the  $\alpha$ -Phase Transformation in  $\text{Si}_3\text{N}_4$ ", *J. Mat. Sci.*, 13 341-50 (1978).
9. C. Greskovich, "Hot-Pressed  $\beta$ - $\text{Si}_3\text{N}_4$  Containing Small Amounts of Be and O in Solid Solutions" *J. Mat. Sci.* 14 2427-38 (1979).
10. F.F. Lange, "High Temperature Strength Behavior of Hot-Pressed  $\text{Si}_3\text{N}_4$ : Evidence For Subcritical Crack Growth", *J. Am. Ceram. Soc.* 57 (2) 84-87 (1974).
11. R. Kossowsky, D.G. Miller and E.S. Diaz, "Tensile and Creep Strengths of Hot-Pressed  $\text{Si}_3\text{N}_4$ ", *J. Mat. Sci.* 10 983-97 (1975).

12. S.U. Din and P.S. Nicholson, "Creep of Hot Pressed  $\text{Si}_3\text{N}_4$ ", *ibid* 10 1375-80 (1975).
13. B.S.B. Karunaratne and M.H. Lewis, "High-Temperature Fracture and Diffusional Deformation Mechanisms in Si-Al-O-N Ceramics", *ibid* 15 449-62 (1980).
14. G.R. Terwilliger and F.F. Lange, "Pressureless Sintering of Silicon Nitride, *ibid* 10 1169-74 (1975).
15. M. Mitomo, "Pressure Sintering of  $\text{Si}_3\text{N}_4$ ", *ibid* 11, 1103-07 (1976).
16. C. Greskovich and J.A. Palm, "Development of High Performance Sintered  $\text{Si}_3\text{N}_4$ ", Final Technical Report, September 1980, Contract No. DAAG46-78-C-0058.
17. W.D. Pasco and C.D. Greskovich, "Sintered  $\text{Si}_3\text{N}_4$  for High Performance Thermomechanical Applications," Final Technical Report, April 1982, Contract No. DAAG46-81-C-0029.
18. D.R. Clarke and F.F. Lange, "Oxidation of  $\text{Si}_3\text{N}_4$  Alloys: Relation to Phase Equilibria in the System  $\text{Si}_3\text{N}_4$ - $\text{SiO}_2$ - $\text{MgO}$ ", *J. Am. Ceram. Soc.* 63, 9-10, 586-93 (1980).
19. J. Lankford, "Indentation Microfracture in the Palmqvist Crack Regime: Implications for Fracture Toughness Evaluation by the Indentation Method", *J. Mat. Sci. Let.* 1, p.493-95, (1982).
20. I.C. Huseby, H.L. Lukas and G. Petzow, "Phase Equilibria in the System  $\text{Si}_3\text{N}_4$ - $\text{SiO}_2$ - $\text{BeO}$ - $\text{Be}_3\text{N}_2$ ", *J. Am. Ceram. Soc.* 58 (9-10) 377-80 (1975).
21. G.E. Gazza, Influence of Composition and Process Selection on Densification of Silicon Nitride," Report # AMMRC-TR-82-32, (1982).
22. "Process for Producing Metallic Nitride Powder", U.S. Pat. 4,196,178, (1980).

TABLE I

Comparison of Properties of Small and Large Samples of GPS Si<sub>3</sub>N<sub>4</sub>

|                    |        | <u>Small(0.2x0.2x1.9cm)</u>   | <u>Large(0.6x0.6x3.8cm)</u>   |
|--------------------|--------|---|---|
| Modulus of Rupture | 25°C   | 597 MPa(m=8.3)  | 440 MPa(m=7.8)  |
|                    | 1300°C | 553 MPa(m=12.9)   | NA  |
|                    | 1400°C | NA  | 410   |
|                    | 1500°C | NA  | 279   |
| Creep              | 1300°C | 4.6x10 <sup>-7</sup> h <sup>-1</sup> (69 MPa)                       | 2x10 <sup>-6</sup> h <sup>-1</sup> (345 MPa)                          |
|                    | 1400°C | 6.9x10 <sup>-6</sup> h <sup>-1</sup> (69 MPa)                       | 4x10 <sup>-5</sup> h <sup>-1</sup> (207 MPa)                          |
| Oxidation          | 1300°C | 1x10 <sup>-12</sup> kg <sup>2</sup> m <sup>-4</sup> S <sup>-1</sup> | 7.4x10 <sup>-13</sup> kg <sup>2</sup> m <sup>-4</sup> S <sup>-1</sup> |
|                    | 1400°C | NA  | 2.1x10 <sup>-12</sup> kg <sup>2</sup> m <sup>-4</sup> S <sup>-1</sup> |
|                    | 1500°C | 6x10 <sup>-12</sup> kg <sup>2</sup> m <sup>-4</sup> S <sup>-1</sup> | NA  |
| K <sub>IC</sub>    |        | 2.9 MNn <sup>-3/2</sup>   |   |
| VHN (500g load)    |        | 1650kg/mm <sup>2</sup>  |   |

Table II  
Sintering Behavior of  $\text{Si}_3\text{N}_4$  Containing  $\text{BeSiN}_2$  and  $\text{Y}_2\text{O}_3$  Additives

| <u>w/o BeSiN<sub>2</sub></u> | <u>w/o Y<sub>2</sub>O<sub>3</sub></u> | <u>Δw/w<sub>0</sub> %</u> | <u>w/o Oxygen</u> | <u>% ρ<sub>th</sub></u> |
|------------------------------|---------------------------------------|---------------------------|-------------------|-------------------------|
| 1.0                          | 0                                     | -2.5                      | 1.86              | 57.9                    |
| 1.0                          | 1.0                                   | -1.52                     | 2.07              | 82.2                    |
| 1.0                          | 2.0                                   | -1.25                     | 2.29              | 84.5                    |
| 1.0                          | 3.0                                   | -1.07                     | 2.50              | 84.2                    |
| 2.0                          | 0                                     | -0.77                     | 1.86              | 56.9                    |
| 2.0                          | 1.0                                   | -0.25                     | 2.07              | 83.0                    |
| 2.0                          | 2.0                                   | +0.23                     | 2.29              | 95.0                    |
| 2.0                          | 3.0                                   | -0.40                     | 2.50              | 93.2                    |
| 3.0                          | 0                                     | -0.31                     | 1.86              | 56.9                    |
| 3.0                          | 1.0                                   | +0.14                     | 2.07              | 98.8                    |
| 3.0                          | 2.0                                   | +0.65                     | 2.29              | 99.4                    |
| 3.0                          | 3.0                                   | +0.71                     | 2.50              | 99.1                    |

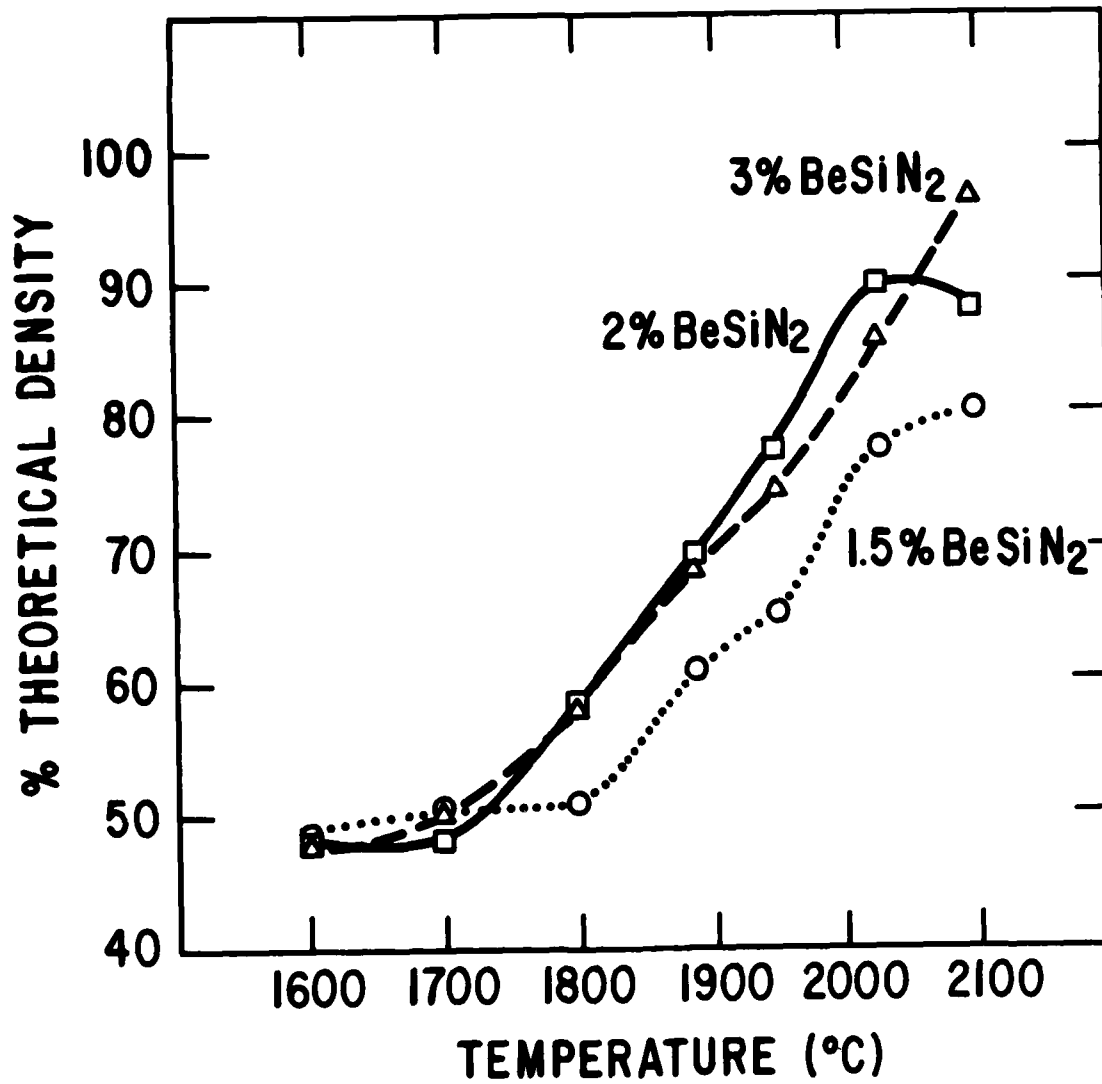


Figure 1 Densification Behavior as a Function of Temperature for the (1.5,2), (2,2) and (3,2) Compositions

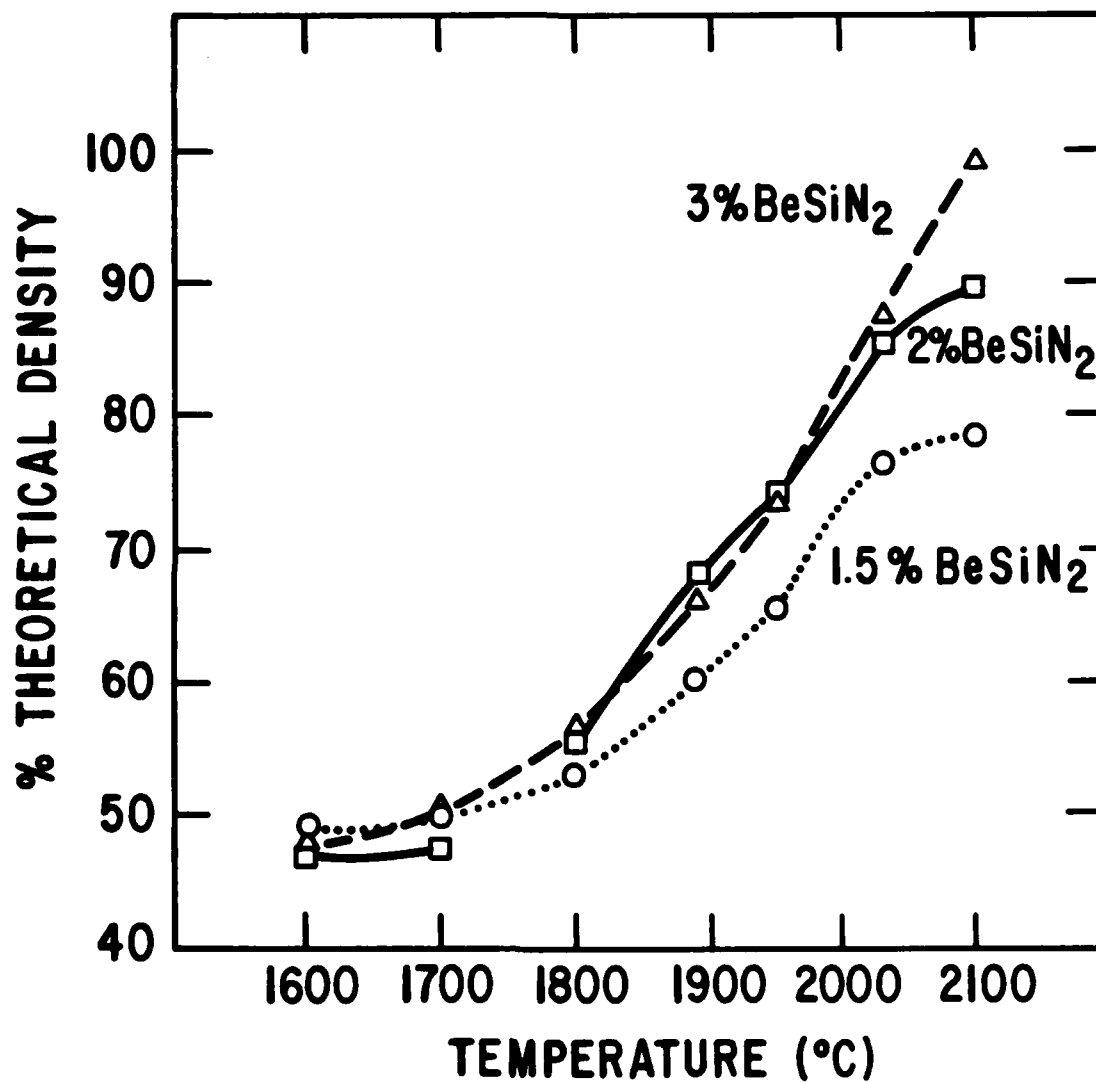


Figure 2 Densification Behavior as a Function of Temperature for the (1.5, 3) (2,3) and (3,3) Compositions

Table III  
Weight Change During Sintering as a Function of Temperature  
for  $\text{Si}_3\text{N}_4$  Containing  $\text{BeSiN}_2$  and  $\text{Y}_2\text{O}_3$  Additives

| <u>Temp. °C</u> | <u>1.5/2</u> | <u>2/2</u> | <u>3/2</u> | <u>1.5/3</u> | <u>2/3</u> | <u>3/3</u> |
|-----------------|--------------|------------|------------|--------------|------------|------------|
| 1600            | 0.56         | 0.47       | 0.44       | 0.47         | 0.45       | 0.40       |
| 1700            | 0.52         | 0.45       | 0.47       | 0.44         | 0.50       | 0.44       |
| 1800            | 0.30         | 0.33       | 0.39       | 0.35         | 0.57       | 0.45       |
| 1875            | 0.02         | 0.16       | 0.23       | 0.34         | 0.68       | 0.54       |
| 1950            | -0.03        | -0.01      | 0.22       | 0.11         | 0.78       | 0.37       |
| 2030            | -0.50        | -0.16      | -0.05      | -0.18        | 0.51       | 0.27       |

Table IV  
 Phases Present as a Function of Temperature  
 for the "Grain Boundary Composition"

| <u>Temperature °C</u> | <u>Phases Present</u>  |
|-----------------------|--|
| 1400                  | BeSiN <sub>2</sub> , Si <sub>2</sub> N <sub>2</sub> O, Y <sub>2</sub> Si <sub>2</sub> O <sub>7</sub> ,<br>Be <sub>2</sub> Y <sub>2</sub> SiO <sub>7</sub> Liquid |
| 1500                  | Si <sub>2</sub> N <sub>2</sub> O, Be <sub>2</sub> Y <sub>2</sub> SiO <sub>7</sub> , Liquid   |
| 1600                  | β-Si <sub>3</sub> N <sub>4</sub> , Be <sub>2</sub> Y <sub>2</sub> SiO <sub>7</sub> , Y <sub>2</sub> Si <sub>2</sub> O <sub>7</sub> , Liquid                      |
| 1700                  | β-Si <sub>3</sub> N <sub>4</sub> , trace Be <sub>2</sub> Y <sub>2</sub> SiO <sub>7</sub> ,<br>Y <sub>2</sub> Si <sub>2</sub> O <sub>7</sub> Liquid               |
| 1900                  | β-Si <sub>3</sub> N <sub>4</sub> , Liquid  |
| 2050                  | β-Si <sub>3</sub> N <sub>4</sub> , Liquid  |

TABLE V

Optimization of the Sintering Process for  $\text{Si}_3\text{N}_4$   
Containing  $\text{BeSiN}_2$  and  $\text{Y}_2\text{O}_3$  Additives

| <u>Sample #</u> | <u>Crucible</u> | <u>Sintering Conditions T, t, P</u>   | <u><math>\rho</math> g/cm<sup>3</sup></u> | <u><math>\Delta W/W_0</math> %</u> |
|-----------------|-----------------|---|---|------------------------------------|
| SNBY 2.5, 3 - 1 | BN              | 1700°C, 30 min 250 psi<br>2050°C, 30 min, 300 psi<br>1950°C, 30 min, 1000 psi       | 3.18                                      | -0.17                              |
| - 2             | BN              | 1700°C, 30 min, 250 psi<br>2050°C, 30 min, 3000 psi                                 | 3.11                                      | -0.15                              |
| - 3             | BN              | 1910°C, 30 min, 280 psi<br>2045°C, 30 min, 300 psi                                  | 3.17                                      | +0.12                              |
| - 4             | RBSN            | 1700°C, 30 min, 250 psi<br>2025°C, 30 min, 300 psi<br>1950°C, 30 min, 1000 psi      | 3.23                                      | -0.10                              |
| - 5             | RBSN            | 1700+1900°C, 30 min 250 psi<br>2020°C, 30 min, 300 psi<br>1950°C, 30 min, 1000 psi  | 3.23                                      |                                    |
| - 6             | RBSN            | Same 5  | 3.21                                      | -0.47                              |
| - 7             | RBSN            | 1700°C, 30 min, 260 psi<br>2030°C, 30 min, 300 psi<br>1950°C, 30 min, 1000 psi      | 3.22                                      | -0.43                              |
| - 8             | RBSN            | 1700+1900°C, 30 min, 260 psi<br>2020°C, 15 min, 300 psi<br>1950°C, 30 min, 1000 psi | 3.21                                      | -0.51                              |

TABLE VI

Room Temperature MOR Of the (2.5, 3) and (3,3) Compositions

| <u>Sample #</u> | <u>%<math>\rho</math></u> | <u>W (cm)</u> | <u>h (cm)</u> | <u>MOR (MPa)</u> |
|-----------------|---------------------------|---------------|---------------|------------------|
| (2.5, 3) - 1    | 99.5                      | 0.638         | 0.505         | 740              |
| -2              | 99.5                      | 0.638         | 0.505         | 490              |
| -3              | 99.5                      | 0.638         | 0.505         | 690              |
| -4              | 99.5                      | 0.638         | 0.505         | 726              |
| -5              | 99.5                      | 0.638         | 0.505         | 796              |
| -6              | 99.5                      | 0.638         | 0.505         | 708              |
| (3,3) -1        | 99.7                      | 0.638         | 0.513         | 641              |
| -2              | 99.7                      | 0.638         | 0.513         | 549              |
| -3              | 99.7                      | 0.638         | 0.513         | 585              |
| -4              | 99.7                      | 0.638         | 0.513         | 578              |
| -5              | 99.7                      | 0.638         | 0.513         | 457              |
| -6              | 99.7                      | 0.638         | 0.513         | 486              |

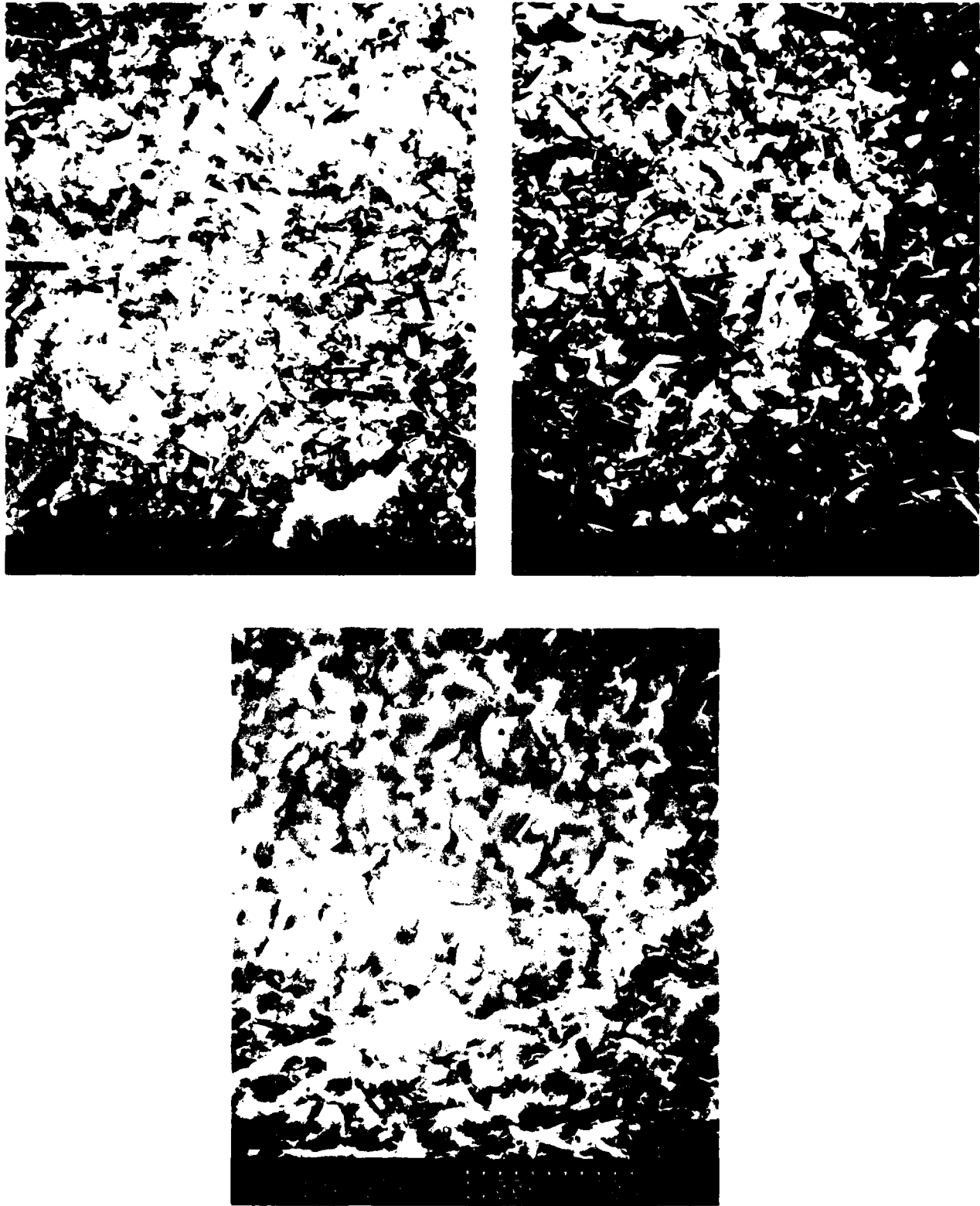


Figure 3 Fracture Surfaces of the (a) (2.5, 3) Composition, (b) (3,3) Composition, and (c) Baseline Composition

TABLE VII

Steady State Creep Rates of the (2.5, 3) and (3,3) Compositions

| <u>Composition</u> | <u>1200°C</u>         | <u>1300°C</u>         | <u>1350°C</u>         |
|--------------------|-----------------------|-----------------------|-----------------------|
| (2.5, 3)           |                       | $4.23 \times 10^{-5}$ | $7.68 \times 10^{-4}$ |
| (2.5, 3) HT        | $8.75 \times 10^{-7}$ | $3.58 \times 10^{-5}$ | $1.65 \times 10^{-4}$ |
| (3, 3)             | $1.16 \times 10^{-6}$ | $7.17 \times 10^{-5}$ | $6.75 \times 10^{-4}$ |

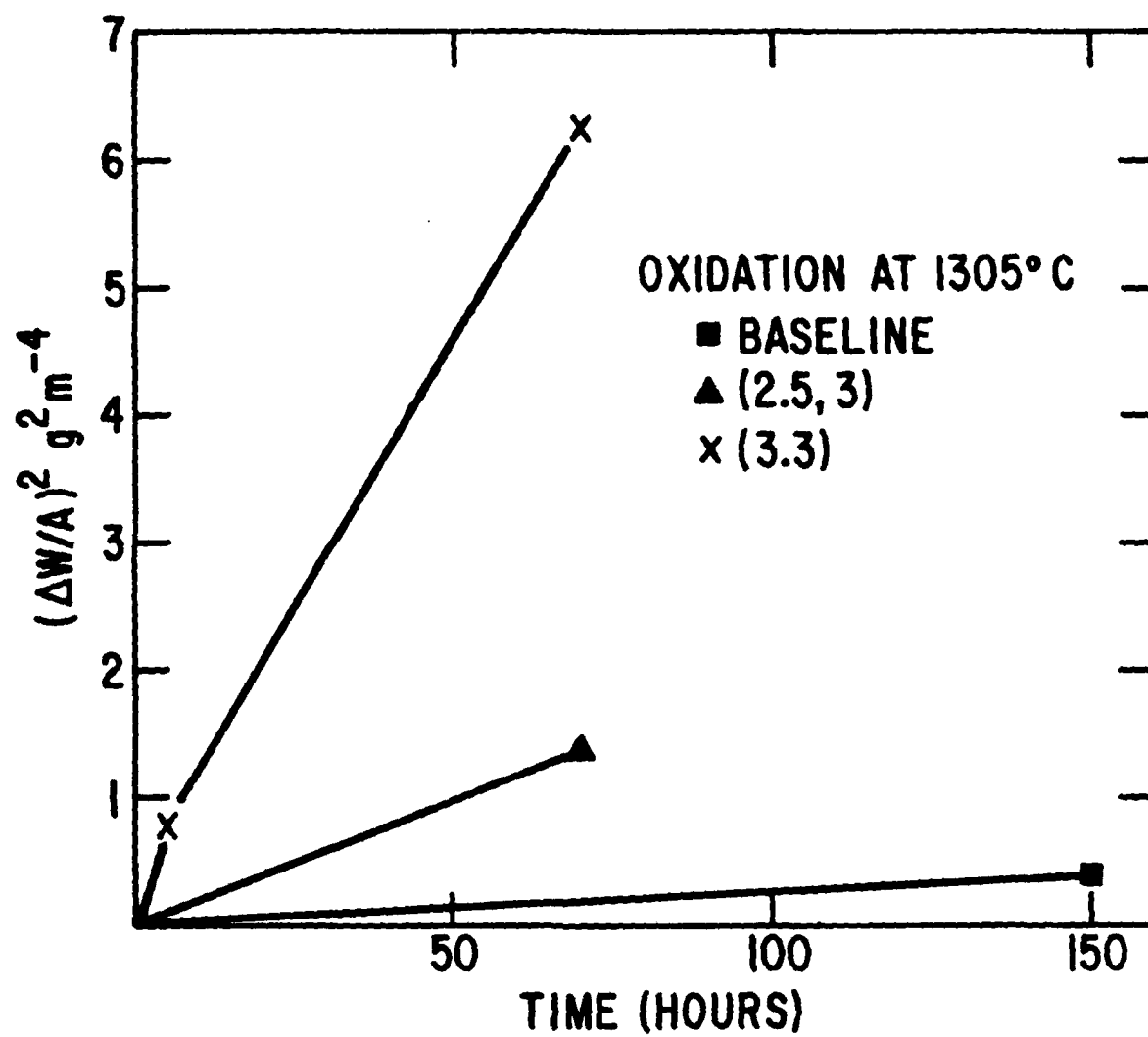


Figure 4 Oxidation Behavior of the (2.5, 3) (3,3) and Baseline Compositions at 1300°C in Flowing Oxygen

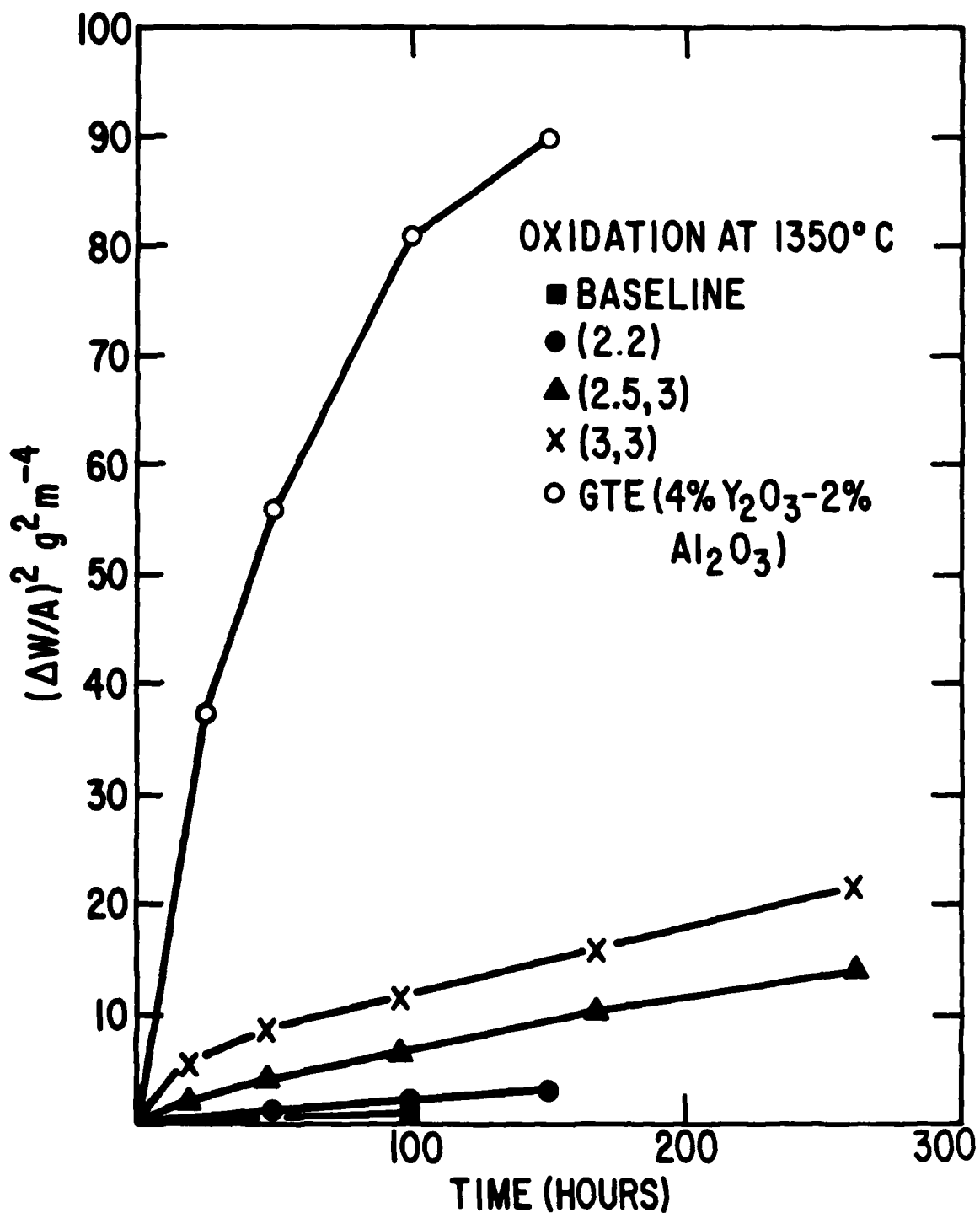
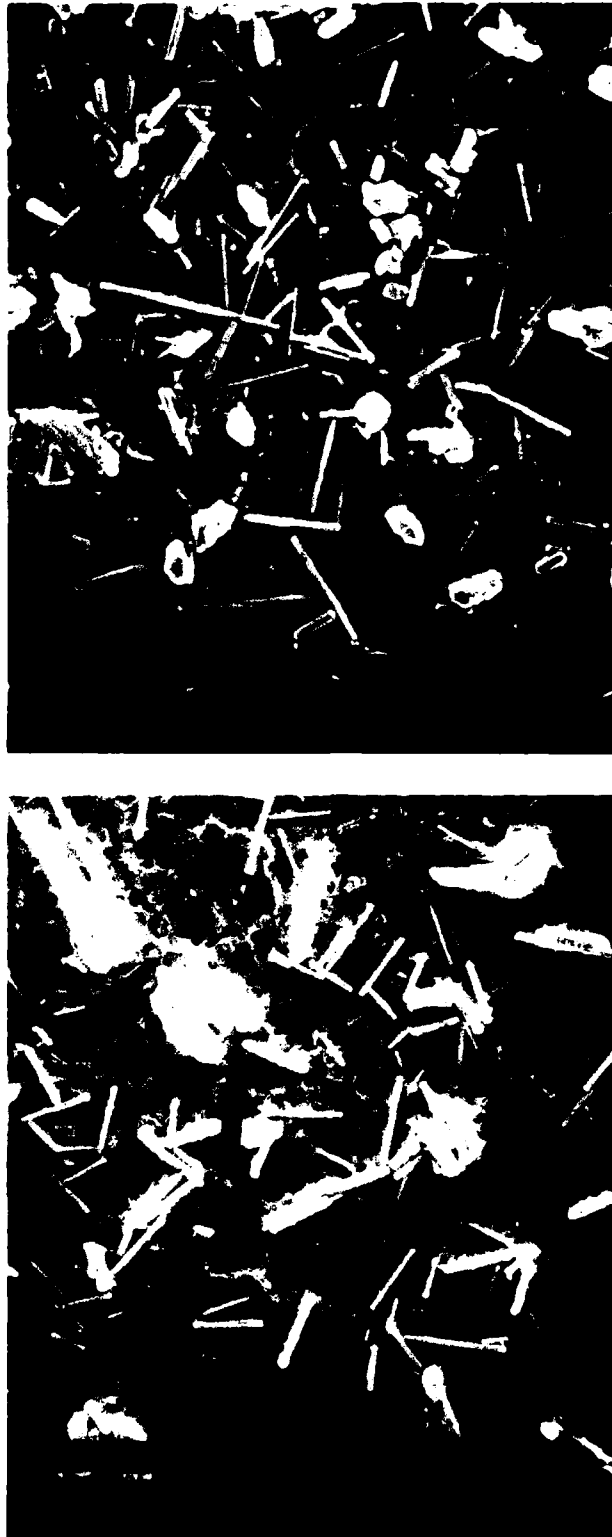


Figure 5

Oxidation Behavior of the (2.5,3) (3,3), Baseline and GTE Sylvania Compositions at 1350°C in Flow Oxygen



**Figure 6** SEM Micrographs of Oxidized Surfaces of the (a) (2.5, 3) and (b) (3,3) Compositions

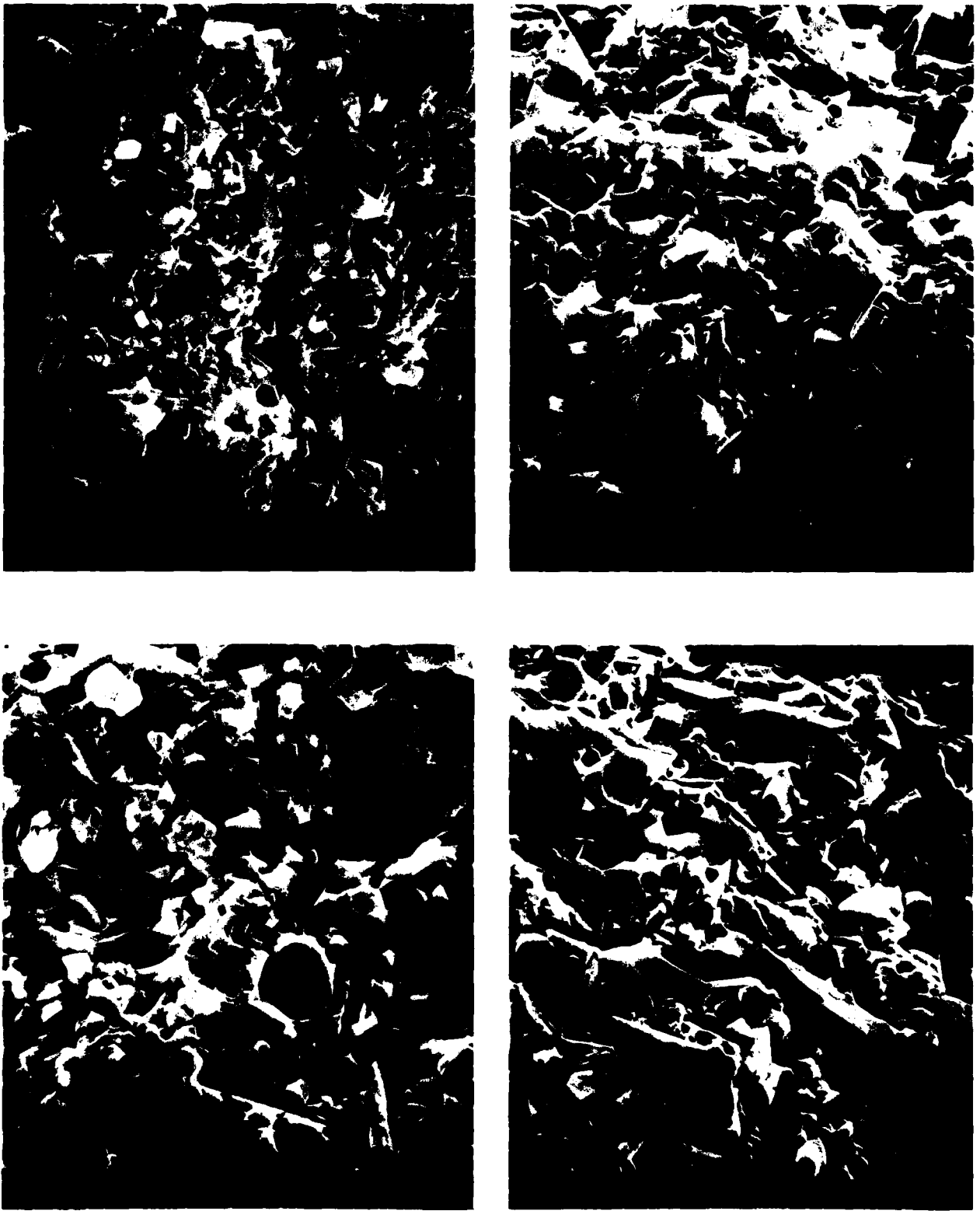
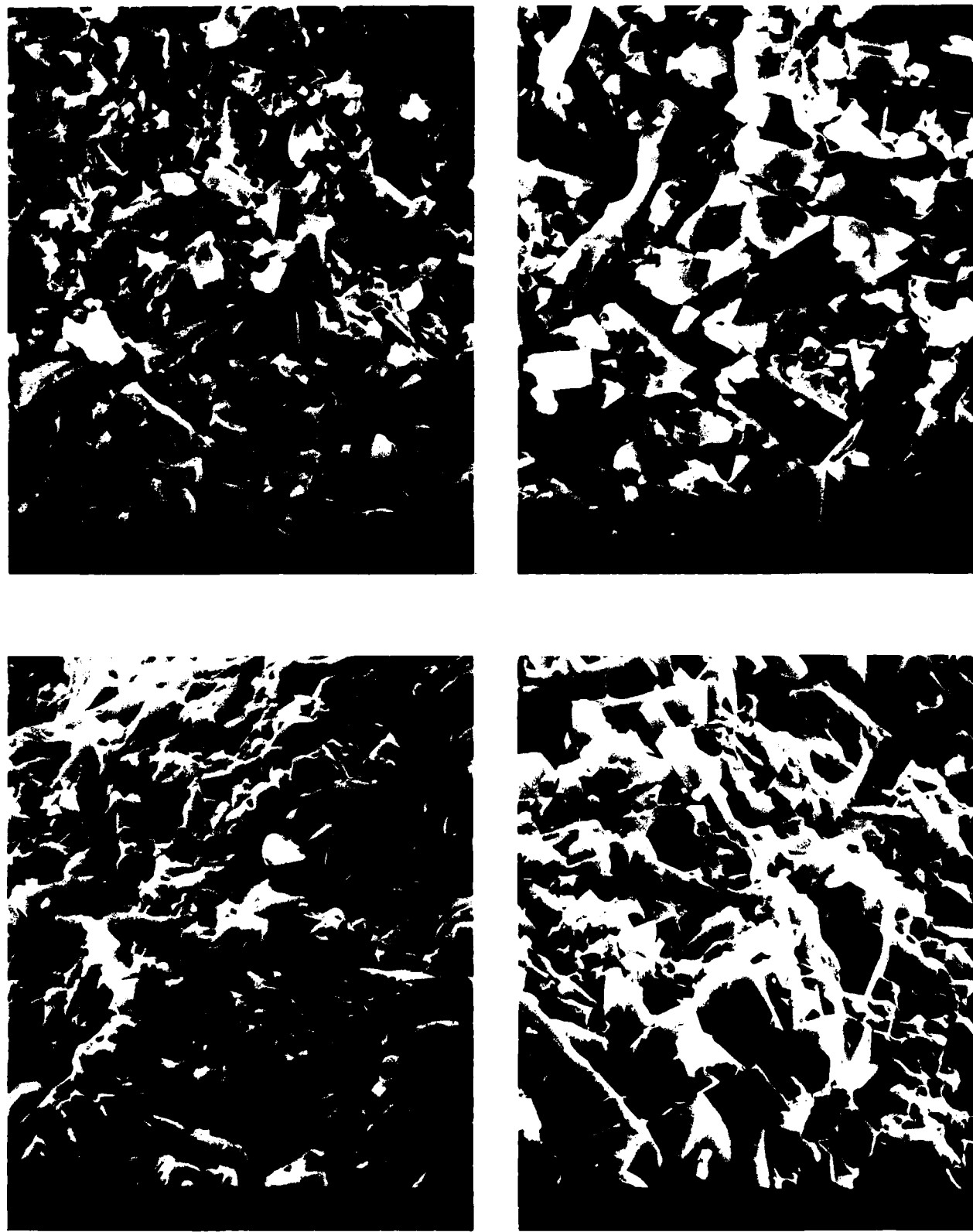


Figure 7 SEM Micrographs of Fracture Surfaces of (a) the (2.5, 3) Composition Fired at  $2025^{\circ}\text{C}$  (b) the (3,3) Composition Fired at  $2025^{\circ}\text{C}$ , (c) the (2.5, 3) Composition Fired at  $2050^{\circ}\text{C}$ , and (d) the (3,3) Composition Fired at  $2050^{\circ}\text{C}$



**Figure 8** SEM Micrographs of Fracture Surface of (a) the (2,2) Composition (b) the (2.5, 2.5) Composition, (c) the (3,4) Composition and (d) the (4,3) Composition Fired at 2050°C.

TABLE VIII

Phase Present as a Function of Composition After GPS at 2050°C

| <u>Composition</u> | <u>Phases Present</u>         |  |
|--------------------|-------------------------------|--|
|                    | <u>MAJOR</u>                  | <u>MINOR</u>   |
| (2, 2)             | $\beta\text{-Si}_3\text{N}_4$ | $\text{Be}_2\text{Y}_2\text{SiO}_7, \text{Y}_2\text{SiO}_7$          |
| (2.5, 2.5)         | $\beta\text{-Si}_3\text{N}_4$ | $\text{Be}_2\text{Y}_2\text{SiO}_7, \text{Y}_2\text{Si}_2\text{O}_7$ |
| (2.5, 3)           | $\beta\text{-Si}_3\text{N}_4$ | $\text{Be}_2\text{Y}_2\text{SiO}_7, \text{Y}_2\text{Si}_2\text{O}_7$ |
| (3, 3)             | $\beta\text{-Si}_3\text{N}_4$ | $\text{Be}_2\text{Y}_2\text{SiO}_7, \text{Y}_2\text{Si}_2\text{O}_7$ |
| (3, 4)             | $\beta\text{-Si}_3\text{N}_4$ | $\text{Y}_2\text{Si}_2\text{O}_7$                                    |
| (4, 3)             | $\beta\text{-Si}_3\text{N}_4$ | $\text{Y}_2\text{Si}_2\text{O}_7$                                    |

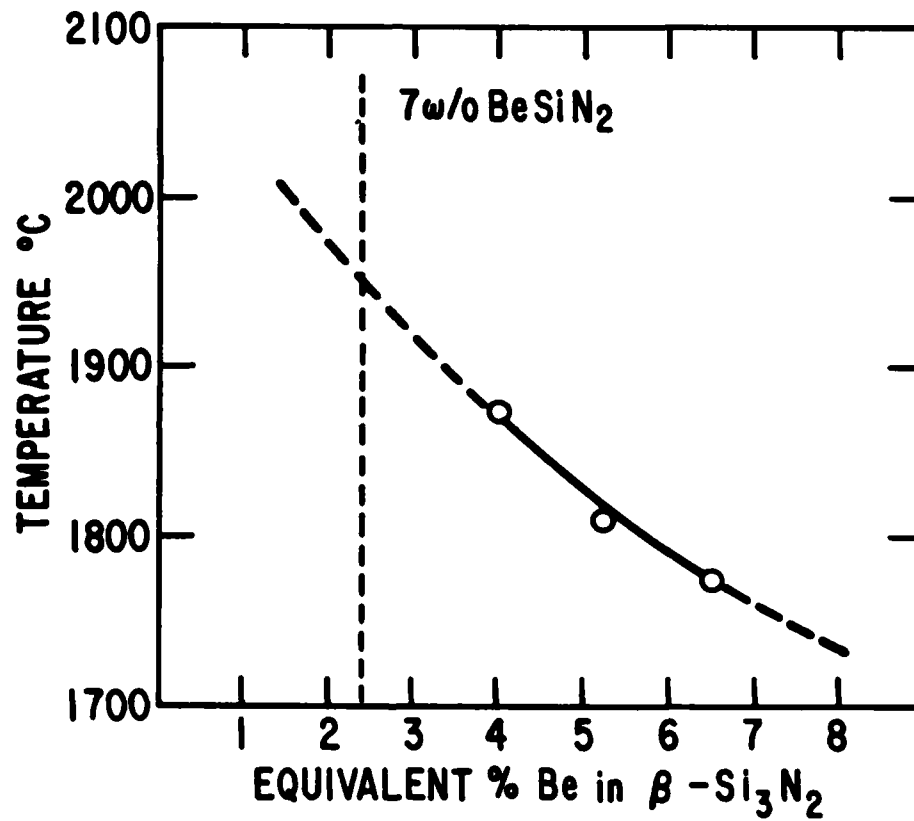


Figure 9 Plot of Be Solubility in  $\beta$ -Si<sub>3</sub>N<sub>4</sub> versus Temperatures as Reported by Huseby et al.<sup>(20)</sup>

TABLE IX

Densification of  $\text{Si}_3\text{N}_4$  Containing  $\text{LiAl}_5\text{O}_8$  and  $\text{YF}_3$  Additives

| <u>Additive</u>  | <u>Sintering Conditions T, t, P</u> | <u>%<math>\rho</math></u> | <u>% <math>\text{O}_2</math></u> | <u>% w/wo</u> |
|--|-------------------------------------|---------------------------|----------------------------------|---------------|
| 5 w/o $\text{LiAl}_5\text{O}_8$                          | 1660°C, 2 h, 1.7 MPa                | 82.7                      | 3.9                              | -0.6          |
|  | 1720°C, 2 h, 1.7 MPa                | 86.2                      | 3.9                              | -0.6          |
|  | 1810°C, 1 h, 1.7 MPa                | 87.1                      | 3.9                              | -0.9          |
|  | 1920°C, 1 h, 1.9 MPa                | 88.1                      | 3.9                              | -1.2          |
| 5 w/o $\text{LiAl}_5\text{O}_8$                          | 1705°C, 4 h, 1.8 MPa                | 84.3                      | 6.5                              | -1.8          |
| 5 w/o $\text{LiAl}_5\text{O}_8$                          | 1820°C, 1 h, 1.9 MPa                | 88.1                      | 7.9                              | -0.5          |
| 5 w/o $\text{LiAl}_5\text{O}_8$<br>- 3 w/o $\text{YF}_3$ | 1700°C, 1 h, 1.7 MPa                | 87.0                      | 3.9                              | -2.8          |
|  | 1800°C, 3 h, 1.9 MPa                | 96.0                      | 3.9                              | -4.4          |
|  | 1900°C, 1 h, 1.9 MPa                | 96.0                      | 3.9                              | -4.1          |
|  | 2000°C, 1 h, 2.1 MPa                | 96.9                      | 3.9                              | -4.9          |
| 10 w/o $\text{LiAl}_5\text{O}_8$                         | 1660°C, 2 h, 1.7 MPa                | 89.3                      | 6.2                              | -0.8          |
|  | 1720°C, 2 h, 1.7 MPa                | 90.3                      | 6.2                              | -0.8          |
|  | 1810°C, 1 h, 1.7 MPa                | 87.7                      | 6.2                              | -1.0          |
|  | 1920°C, 1 h, 1.9 MPa                | 84.3                      | 6.2                              | -1.7          |
| 10 w/o $\text{LiAl}_5\text{O}_8$                         | 1705°C, 3 h, 1.8 MPa                | 91.8                      | 7.8                              | -1.1          |
| 10 w/o $\text{LiAl}_5\text{O}_8$                         | 1705°C, 3 h, 1.8 MPa                | 89.0                      | 9.6                              | -1.2          |
| 10 w/o $\text{LiAl}_5\text{O}_8$                         | 1800°C, 3h, 1.7 MPa                 | 84.6                      | 9.1                              |               |
| 10 w/o $\text{LiAl}_5\text{O}_8$                         | 1820°C, 1 h, 1.8 MPa                | 85.5                      | 11.5                             | -1.5          |

TABLE X

Phases Present as a Function of Temperature for  $\text{Si}_3\text{N}_4$   
Containing  $\text{LiAl}_5\text{O}_8$  and  $\text{YF}_3$  Additions

| <u>5 w/o <math>\text{LiAl}_5\text{O}_8</math></u>                            | <u><math>T^\circ\text{C}</math></u> | <u>5 w/o <math>\text{Al}_5\text{O}_8</math> - 3 w/o <math>\text{YF}_3</math></u> |
|--|-------------------------------------|--|
| $\beta$ - $\text{Si}_3\text{N}_4$ , $\alpha$ - $\text{Si}_3\text{N}_4$       | 1700                                | $\beta$ - $\text{Si}_3\text{N}_4$ , minor $\alpha$ - $\text{Si}_3\text{N}_4$     |
| $\beta$ - $\text{Si}_3\text{N}_4$ , $\alpha$ - $\text{Si}_3\text{N}_4$       | 1800                                | $\beta$ - $\text{Si}_3\text{N}_4$  |
| $\beta$ - $\text{Si}_3\text{N}_4$ , trace $\alpha$ - $\text{Si}_3\text{N}_4$ | 1900                                | $\beta$ - $\text{Si}_3\text{N}_4$  |

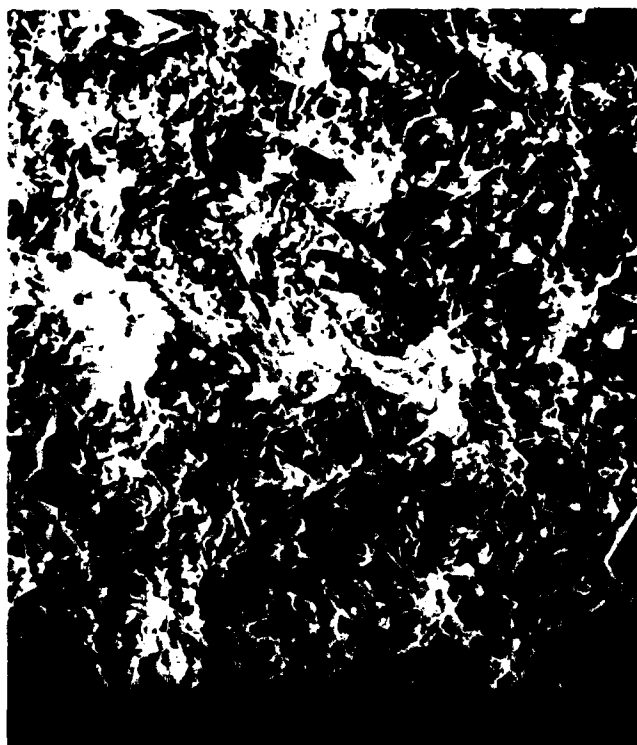


Figure 10 SEM Micrograph of Fracture Surface  $\text{Si}_3\text{N}_4 + 5 \text{ w/o LiAl}_5\text{O}_8 + 3 \text{ w/o YF}_3$

TABLE XI

Densification of  $\text{Si}_3\text{N}_4$  Containing a Variety of Additives

| Additive  | Sintering Conditions T, t, P                | % $\rho$   | % $\text{O}_2$ | % $\Delta w/w_0$ |
|---|---|------------|----------------|------------------|
| 7 w/o $\text{Li}_2\text{SiN}_2$                             | 1850°C, 30 min, 1.7 MPa                     | 53         | 1.8            | -2.1             |
| 7.3 w/o $\text{Ga}_2\text{O}_3$                             | 1900°C, 30 min, 2.1 MPa                     | 53         | 3.7            | -19.6            |
| 1.3 w/o $\text{B}_4\text{C}$<br>+ 0.7 w/o C                 | 2005°C, 30 min, 2.1 MPa                     | Decomposed | 1.8            |                  |
| 10 w/o $\text{ZrO}_2$                                       | 2050°C, 30 min, 6.9 MPa<br>1940°C, 30m, 6.9 | min,<br>70 | 4.4            | 2.2/<br>-13.4    |
| 6.8 w/o $\text{LiAlSiO}_4$                                  | 1710°C, 15 min, 1.7 MPa                     | 67         | 5.5            | -3.7             |
|   | 1950°C, 15 min, 2.2 MPa                     | 70         | 5.5            | -9.4             |
| 5 w/o $\text{LiAlO}_2$                                      | 1800°C, 120 min, 1.9 MPa                    | 77         | 4.4            | -3.5             |
| 10 w/o $\text{LiAlO}_2$                                     | 1800°C, 120 min, 1.9 MPa                    | 76         | 6.9            | -3.8             |
| 5 w/o $\text{LiAlO}_2$<br>+ 3 w/o $\text{YF}_3$             | 1800°C, 120 min, 1.9 MPa                    | 93         | 4.4            | -4.4             |
| 6 w/o $\text{Y}_2\text{O}_3$                                | 1850°C, 60 min, 1.4 MPa                     | 80         | 3.3            | -5.3             |
|   | 1890°C, 50 min, 1.7 MPa                     | 80         | 3.3            | -4.4             |
| 5.7 w/o $\text{Y}_2\text{O}_3$ +<br>11.7 w/o $\text{SiO}_2$ | 1700°C, 120 min, 1.8 MPa                    | 63         | 9.0            | -2.3             |
|   | 1905°C, 120 min, 2.0 MPa                    | 79         | 9.0            | -4.9             |
|   | 1950°C, 120 min, 2.0 MPa                    | 80         | 9.0            | -6.8             |
|   | 2000°C, 120 min, 2.0 MPa                    | 81         | 9.0            | -10.0            |
| 10 w/o YAG  | 2000°C, 30 min, 1.4 MPa                     | 93         | 5.0            | -4.9             |
|   | 2045°C, 30m, 2.2/<br>2000°C, 30m, 6.7       | 97         | 5.0            | -2.9             |

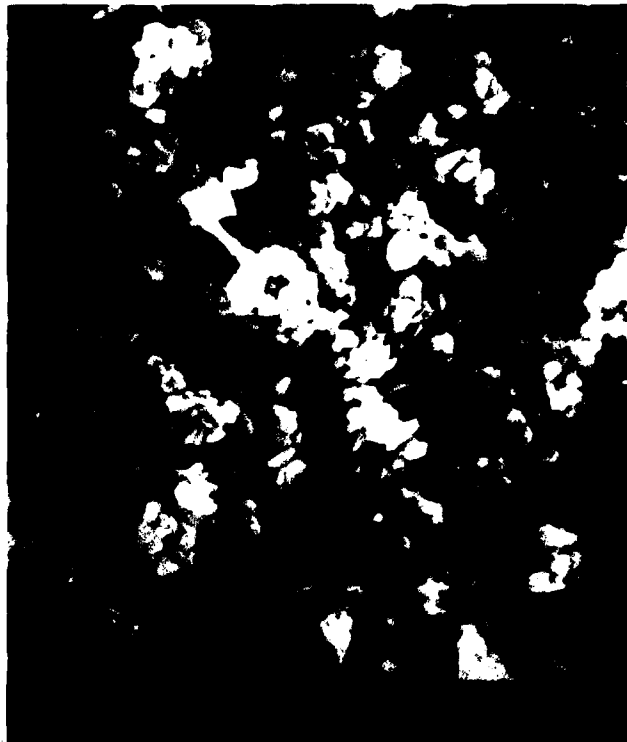


Figure 11 SEM Micrograph Showing Particle Size and Morphology of (a) Ube Industries,  $\text{Si}_3\text{N}_4$  and GTE Sylvania SN502 in the As-received Condition.

TABLE XII

Powder Characterization of Ube-SN-E10  $\text{Si}_3\text{N}_4$ 

| <u>Chemical Analysis</u>                  | <u>Lot A-10</u> | <u>Lot A-18</u> |
|---|-----------------|-----------------|
| N (alkali fusion) wt. %                   | 38              | 38              |
| O (inert gas fusion) wt. %                | 1.2             | 1.4             |
| C (inert gas fusion) wt. %                | NA              | 0.2             |
| Cl (ion electrode) ppm                    | 55              | 70              |
| FE (atomic absorption) ppm                | 200             | 50              |
| CA (atomic absorption) ppm                | 300             | 50              |
| Al (atomic absorption) ppm                | NA              | 50              |
| Specific Surface Area (m <sup>2</sup> /g) | 10              | 12              |
| Tap Density (g/cm <sup>3</sup> )          | 1.0             | 1.0             |
| Degree of crystallinity %                 | 100             | 100             |
| $\beta/\alpha+$ %                         | 3.5             | 2.5             |

TABLE XIII

Densification of Ube  $\text{Si}_3\text{N}_4$ 

| <u>Sample #</u> | <u>Oxygen Content %</u> | <u>Sintering Conditions</u> | <u><math>\rho</math> %</u> | <u><math>\Delta W/W_0</math> %</u> | <u>Crucible</u> | <u>Processing</u> |
|-----------------|-------------------------|-----------------------------|----------------------------|------------------------------------|-----------------|-------------------|
| Ube-001         | 2                       | 1995/30/290-1930/30/1000    | 52.1                       | -3.54                              | BN              | 1                 |
| 002             | 5.1                     | 2005/30/290-1950/30/1000    | 93.2                       | -3.39                              | BN              | 1                 |
| 003             | 3.2                     | 2005/30/290-1950/30/1000    | 93.2                       | -2.45                              | BN              | 1                 |
| 004             | 3.5                     | 2005/30/290-1950/30/1000    | 93.7                       | -2.41                              | BN              | 1                 |
| 005             | 3.4                     | 2065/30/300-1950/30/1000    | 91.6                       | -3.6                               | BN              | 1                 |
| 008             | 3.4                     | 2000/30/290-1950/30/1000    | 96.8                       | -0.87                              | RBSN            | 1                 |
| 009             | 3.4                     | 2020/30/290-1950/30/1000    | 96.6                       | -1.5                               | RBSN            | 1                 |
| 010             | 3.51                    | 2070/30/300-1950/30/1000    | 98.3                       | -2.2                               | RBSN            | 1                 |
| 011             | 3.9                     | 2150/30/310-1950/30/1000    | 91.9                       | -4.7                               | RBSN            | 1                 |
| 013             | 3.8                     | 2085/30/290-1950/30/1000    | 92.7                       | -2.9                               | BN              | 1                 |
| 014             | 3.8                     | 2085/30/295-1950/30/1000    | 79.3                       | -6.0                               | BN              | 1                 |
| 015             | 3.8                     | 2085/30/295-1950/30/1000    | 87.5                       | -3.1                               | BN              | 1                 |
| 016             | ?                       | 2085/30/300-1950/30/1000    | 83.3                       | -5.6                               | RBSN            | 1                 |
| 017             |                         | 2050/30/290-1950/30/1000    | 96.0                       | -0.2                               | BN              | 1                 |
| 018             |                         | 2100/30/300-1950/30/1000    | 97.3                       | -1.0                               | BN              | 1                 |
| 019             | 4.1                     | 2085/30/300-1950/30/1000    | 96.9                       | -2.0                               | BN              | 1                 |
| 022             | 5.3                     | 2050/30/300-1950/30/1000    |                            |                                    | RBSN            | 2                 |
| 023             | 3.9                     | 2050/30/300-1950/30/1000    | 95.9                       | -4.2                               | RBSN            | 2                 |
| 024             | 3.5                     | 2050/30/300-1950/30/1000    | 98.4                       | -1.7                               | BN              | 2                 |
| 025             | 3.5                     | 2100/30/300-1950/30/1000    | 98.4                       | -2.1                               | BN              | 2                 |
| 028             | 3.1                     | 2055/30/300-1950/30/1000    | 98.4                       |                                    | BN              | 3                 |
| 029             | 2.4                     | 2055/30/300-1950/30/1000    | Low density                |                                    | BN              | 3                 |
| 030             | 2.1                     | 2055/30/300-1950/30/1000    | Low density                |                                    | BN              | 3                 |
| 031             | 3.2                     | 2050/30/300-1950/30/1000    | 98.6                       | -1.0                               | BN              | 3                 |

APPENDIX A

This appendix summarizes the patents, reports, papers and presentations that were a direct result of the work done under the DOE program.

## PATENTS

Hot Pressing of Silicon Nitride Using Magnesium Silicide, U.S. Patent 4,093,687.

Sintering of Silicon Nitride Using Mg and Be Additives, U.S. Patent 4,119,475.

Sintering of Silicon Nitride Using Be Additive, U.S. Patent 4,119,689.

Sintering of Silicon Nitride Using Mg and Be Additives, U.S. Patent 4,119,690.

Hot Pressing of Silicon Nitride Using Beryllium Additive, U.S. Patent 4,112,140.

Preparation of Silicon Nitride Powder, U.S. Patent 4,112,155.

Hot Pressing of Silicon Nitride Using Magnesium Silicide, U.S. Patent 4,124,402.

Hot Pressing of Silicon Nitride Using Beryllium Additive, U.S. Patent 4,124,403.

Sintering of Silicon Nitride Using Be Additive, U.S. Patent 4,225,356.

Light-Transmitting Silicon Nitride, U.S. Patent 4,279,656,

Light-Transmitting Silicon Nitride, U.S. Patent 4,279,657.

Sintering of Silicon Nitride to High Density, U.S. Patent 4,379,110.

Sintering of Silicon Nitride with Be Additive, U.S. Patent 4,374,792.

## REPORTS

1. S. Prochazka and C. D. Greskovich, "Development of a Sintering Process for High Performance Silicon Nitride," Final Technical Report AMMRC #TR-78-32, 1978.
2. C. D. Greskovich and J. A. Palm, "Development of High Performance Sintered  $\text{Si}_3\text{N}_4$ ," Final Technical Report AMMRC #TR-80-46, 1980.
3. W. D. Pasco and C. D. Greskovich, "Sintered  $\text{Si}_3\text{N}_4$  for High Performance Thermomechanical Applications," Final Technical Report AMMRC #TR-82-22, 1982.
4. W. D. Pasco, "Development of Sintered  $\text{Si}_3\text{N}_4$  for High Performance Thermomechanical Applications," Final Technical Report AMMRC #TR-84-4.

## PAPERS

1. C. Greskovich and S. Prochazka, "Observations on the  $\alpha \rightarrow \beta$   $\text{Si}_3\text{N}_4$  Transformation," J. Am. Ceram. Soc. 60 [9-10] 471-72 (1977).
2. S. Prochazka and C. Greskovich, "Synthesis and Characterization of a Pure Silicon Nitride Powder," Am. Ceram. Soc. Bull. 57 [6] 579-82 (1978).
3. S. Prochazka and C. Greskovich, "Effect of Some Impurities on Sintering  $\text{Si}_3\text{N}_4$ ," Proc. of International Symp. of Factors in Densification and Sintering of Oxide and Non-oxide Ceramics, (1978).
4. C. Greskovich and J. A. Palm, "Observations on the Fracture Toughness of  $\beta$ - $\text{Si}_3\text{N}_4$ - $\beta$ -SiC Composites," Am. Ceram. Soc. Bull. 63 [9-10] 597-599 (1980).
5. C. Greskovich, "Microstructural Observations on Hot-Pressed  $\text{Si}_3\text{N}_4$ ," J. Am. Ceram. Soc. 64 [2] C-31 (1981).
6. C. Greskovich and S. Prochazka, "Stability of  $\text{Si}_3\text{N}_4$  and Liquid Phase(s) During Sintering," J. Am. Ceram. Soc. 64 [7] C96-97 (1981).
7. C. Greskovich, "Preparation of High Density  $\text{Si}_3\text{N}_4$  By A Gas-Pressure Sintering Process," J. Am. Ceram. Soc. 64 [12] 725-30 (1981).
8. R. N. Katz, G. E. Gazza and C. D. Greskovich, "Sintered Silicon Nitride," 5th Int. Symp. on Automotive Propulsion Systems, Conf. 800419 Vol. 1, (1980).
9. W. D. Pasco and C. D. Greskovich, "Sintered  $\text{Si}_3\text{N}_4$  for High Performance Thermomechanical Applications," Proc. of 20th ATDCCM, SAE P120, (1982).
10. C. Greskovich, W. D. Pasco and G. D. Quinn, "Thermomechanical Properties of a New Composition of Sintered  $\text{Si}_3\text{N}_4$ ," Accepted by J. Am. Ceram. Soc. (1984).
11. W. D. Pasco and D. G. Polensky, "Sintering and Properties of  $\text{Si}_3\text{N}_4$  Containing  $\text{SiBeN}_2$  and  $\text{Y}_2\text{O}_3$  Additives," To be submitted to J. Am. Ceram. Soc.

## PRESENTATIONS

C. D. Greskovich and S. Prochazka, "Effect of Impurities on Sintering  $\text{Si}_3\text{N}_4$ ," International Conference on Factors Affecting the Densification of Ceramics, Hakone, Japan, October 1978.

C. D. Greskovich and S. Prochazka, "Some Aspects of Sintering  $\text{Si}_3\text{N}_4$ ," Toshiba Research Center, Kawasaki, Japan, October 1978.

C. D. Greskovich, "Development of High Performance Sintered  $\text{Si}_3\text{N}_4$ ," ATD/CCM, Dearborn, MI, October 1979.

R. N. Katz, G. E. Gazza and C. D. Greskovich, "Sintered Silicon Nitride," 5th International Symposium on Automotive Propulsion Systems, Dearborn, MI, April 1980.

C. D. Greskovich, "Controlling the Oxygen Content of  $\text{Si}_3\text{N}_4$  Powder," Annual Meeting of the American Ceramic Society, Chicago, IL, April 1980.

C. D. Greskovich, "Sintering  $\text{Si}_3\text{N}_4$  to High Density," Annual Meeting of the American Ceramic Society, Washington, DC, May 1981.

C. D. Greskovich, "A Gas Pressure Sintering Process for  $\text{Si}_3\text{N}_4$  Ceramics," NATO-ASI Nitrogen Ceramics Conference, Brighton, England, July 1981.

C. D. Greskovich, "Sintered  $\text{Si}_3\text{N}_4$  Ceramics," New England Section Meeting on Non-oxide Ceramics, Bass River, MA, October 1981.

W. D. Pasco and C. D. Greskovich, "Sintered  $\text{Si}_3\text{N}_4$  for High Performance Thermomechanical Applications," ATD/CCM, Dearborn, MI, October 1982.

C. D. Greskovich, W. D. Pasco and G. Quinn, "Thermomechanical Properties of a New Composition of Sintered  $\text{Si}_3\text{N}_4$ ," Fulrath Symposium at U. of Cal., Berkeley, October 1983.

C. D. Greskovich, W. D. Pasco and G. Quinn, "Thermomechanical Properties of a New Composition of Sintered  $\text{Si}_3\text{N}_4$ ," Pacific Coast Regional Meeting of American Ceramic Society, San Diego, CA, October 1983.

C. D. Greskovich received the 1983 Fulrath Award based on outstanding contributions to Ceramic Science and engineering for DOE/AMMRC sponsored development work on the "Preparation and Properties of Sintered  $\text{Si}_3\text{N}_4$  Prepared by the 2-Step Gas Pressure Process". Presentations on this subject were given at the following Japanese institutions on January 17-31, 1984:

Tokyo Institute of Technology at the Nagatsuda Campus

Hitachi Research Laboratory in Mito

National Defense Academy in Yokosuka

Asahi Glass Company near Tokyo

NGK Spark Plug Company in Nagoya

Kyoto University, Kyoto

Sumitomo Electric Company at Itami

TDK Ceramics Company, Tokyo.

## DISTRIBUTION LIST

| No. of Copies | To  | No. of Copies | To  |
|---------------|---|---------------|---|
| 1             | Office of the Under Secretary of Defense for Research and Engineering, The Pentagon, Washington, DC 20310                 | 1             | Commander, U.S. Army Test and Evaluation Command, Aberdeen Proving Ground, MD 21005                             |
| 1             | ATTN: Mr. J. Persh  | 1             | ATTN: DRSTE-ME  |
| 1             | Dr. G. Gamota   |               |   |
| 12            | Commander, Defense Technical Information Center, Cameron Station, Building 5, 5010 Duke Street, Alexandria, VA 22314      | 1             | Commander, U.S. Army Foreign Science and Technology Center, 220 7th Street, N.E., Charlottesville, VA 22901     |
| 1             | National Technical Information Service, 5285 Port Royal Road, Springfield, VA 22161                                       | 1             | ATTN: Military Tech, Mr. W. Marley  |
| 1             | Director, Defense Advanced Research Projects Agency, 1400 Wilson Boulevard, Arlington, VA 22209                           | 1             | Commander, Watervliet Arsenal, Watervliet, NY 12189   |
| 1             | ATTN: Dr. A. Bement   | 1             | ATTN: Dr. T. Davidson   |
| 1             | Dr. Van Reuth   | 1             | Director, Eustis Directorate, U.S. Army Mobility Research and Development Laboratory, Fort Eustis, VA 23604     |
| 1             | MAJ Harry Winsor  | 1             | ATTN: Mr. J. Robinson, DAVDL-E-MOS (AVRADCOM)   |
| 1             | Battelle Columbus Laboratories, Metals and Ceramics Information Center, 505 King Avenue, Columbus, OH 43201               | 1             | Naval Research Laboratory, Washington, DC 20375   |
| 1             | ATTN: Mr. Winston Duckworth   | 1             | ATTN: Dr. C. I. Chang - Code 5830   |
| 1             | Dr. D. Niesz  | 1             | Mr. R. Rice   |
| 1             | Deputy Chief of Staff, Research, Development, and Acquisition, Headquarters, Department of the Army, Washington, DC 20301 | 1             | Chief of Naval Research, Arlington, VA 22217  |
| 1             | ATTN: DAMA-PPP, Mr. R. Vawter   | 1             | ATTN: Code 471  |
| 1             | Commander, U.S. Army Medical Research and Development Command, Fort Detrick, Frederick, MD 21701                          | 1             | Dr. A. Diness   |
| 1             | ATTN: SGRD-SI, Mr. Lawrence L. Ware, Jr.  | 1             | Dr. R. Pohanka  |
| 1             | Commander, Army Research Office, P.O. Box 12211, Research Triangle Park, NC 27709   | 1             | Headquarters, Naval Air Systems Command, Washington, DC 20360   |
| 1             | ATTN: Information Processing Office   | 1             | ATTN: Code 5203   |
| 1             | Dr. G. Mayer  | 1             | Code MAT-042M   |
| 1             | Dr. J. Hurt   | 1             | Mr. I. Macklin  |
| 1             | Commander, U.S. Army Materiel Development and Readiness Command, 5001 Eisenhower Avenue, Alexandria, VA 22233             | 1             | Headquarters, Naval Sea Systems Command, 1941 Jefferson Davis Highway, Arlington, VA 22376                      |
| 1             | ATTN: DRCDMD-ST   | 1             | ATTN: Code 035  |
| 1             | DRCLD   | 1             | Commander, Naval Weapons Center, China Lake, CA 93555   |
| 1             | Commander, Harry Diamond Laboratories, 2800 Powder Mill Road, Adelphi, MD 20783   | 1             | ATTN: Mr. F. Markarian  |
| 1             | ATTN: Mr. A. Benderly   | 1             | Commander, U.S. Air Force of Scientific Research, Building 410, Bolling Air Force Base, Washington, DC 20332    |
| 1             | Technical Information Office  | 1             | ATTN: MAJ W. Simmons  |
| 1             | DELHD-RAE   | 1             | Commander, U.S. Air Force Wright Aeronautical Laboratories, Wright-Patterson Air Force Base, OH 45433           |
| 1             | Commander, U.S. Army Missile Command, Redstone Arsenal, AL 35898  | 1             | ATTN: AFWAL/MLLM, Dr. N. Tallan   |
| 1             | ATTN: Technical Library   | 1             | AFWAL/MLLM, Dr. H. Graham   |
| 1             | DRSMI-TB, Redstone Scientific Information Center  | 1             | AFWAL/MLLM, Dr. R. Ruh  |
| 1             | Commander, U.S. Army Aviation Research and Development Command, 4300 Goodfellow Boulevard, St. Louis, MO 63120            | 1             | AFWAL/MLLM, Dr. A. Katz   |
| 1             | ATTN: DRDAV-EGX   | 1             | AFWAL/MLLM, Mr. K. S. Mazdidasni  |
| 1             | DRDAV-QE  | 1             | Aero Propulsion Labs, Mr. R. Marsh  |
| 1             | Technical Library   | 1             | National Aeronautics and Space Administration, Washington, DC 20546   |
| 1             | Commander, U.S. Army Tank-Automotive Command, Warren, MI 48090  | 1             | ATTN: Mr. G. C. Deutsch - Code RW   |
| 1             | ATTN: Dr. W. Bryzik   | 1             | Mr. J. Gangler  |
| 1             | Mr. E. Hamperian  | 1             | AFSS-AD, Office of Scientific and Technical Information   |
| 1             | D. Rose   | 1             | National Aeronautics and Space Administration, Lewis Research Center, 21000 Brookpark Road, Cleveland, OH 44135 |
| 1             | DRSTA-RKA   | 1             | ATTN: J. Accurio, USAMRDL   |
| 1             | DRSTA-UL, Technical Library   | 1             | Dr. H. B. Probst, MS 49-1   |
| 1             | DRSTA-R   | 1             | Dr. S. Dutta  |
| 1             | Commander, U.S. Army Armament Research and Development Command, Dover, NJ 07801   | 1             | Mr. S. Grisaffe   |
| 1             | ATTN: Dr. G. Vezzoli  | 1             | National Aeronautics and Space Administration, Langley Research Center, Hampton, VA 23665                       |
| 1             | Mr. Harry E. Peibly, Jr., PLASTECH, Director  | 1             | ATTN: Mr. J. Buckley, Mail Stop 387   |
| 1             | Technical Library   | 1             | Department of Energy, Division of Transportation, 20 Massachusetts Avenue, N.W., Washington, DC 20545           |
| 1             | Commander, U.S. Army Armament Materiel Readiness Command, Rock Island, IL 61299   | 1             | ATTN: Mr. George Thur (TEC)   |
| 1             | ATTN: Technical Library   | 1             | Mr. Robert Schulz (TEC)   |
| 1             | Commander, Aberdeen Proving Ground, MD 21005  | 1             | Mr. John Neal (CLNRT)   |
| 1             | ATTN: DRDAR-CLB-PS, Mr. J. Vervier  | 1             | Department of Transportation, 400 Seventh Street, S.W., Washington, DC 20590                                    |
| 1             | Commander, U.S. Army Mobility Equipment Research and Development Command, Fort Belvoir, VA 22060                          | 1             | ATTN: Mr. M. Lauriente  |
| 1             | ATTN: DRDME-EM, Mr. W. McGovern   | 1             | National Research Council, National Materials Advisory Board, 2101 Constitution Avenue, Washington, DC 20418    |
| 1             | DRDME-V, Mr. E. York  | 1             | ATTN: D. Groves   |
| 1             | Director, U.S. Army Ballistic Research Laboratory, Aberdeen Proving Ground, MD 21005                                      | 1             | R. M. Spriggs   |
| 1             | ATTN: DRDAR-TSB-S (STINFO)  | 1             | National Science Foundation, Washington, DC 20550   |
|               |   | 1             | ATTN: B. A. Wilcox  |
|               |   | 1             | Admiralty Materials Technology Establishment, Polle, Dorset BH16 6JU, UK  |
|               |   | 1             | ATTN: Dr. D. Godfrey  |
|               |   | 1             | Dr. M. Lindley  |

| No. of Copies | To  | No. of Copies | To  |
|---------------|---|---------------|---|
| 1             | AiResearch Manufacturing Company, AiResearch Casting Company, 2525 West 190th Street, Torrance, CA 90505<br>ATTN: Mr. K. Styhr  | 1             | Midwest Research Institute, 425 Volker Boulevard, Kansas City, MO 64110<br>ATTN: Mr. Gordon W. Gross, Head, Physics Station   |
| 1             | AiResearch Manufacturing Company, Materials Engineering Dept., 111 South 34th Street, P.O. Box 5217, Phoenix, AZ 85010<br>ATTN: Mr. D. W. Richerson, MS 93-393/503-44             | 1             | Norton Company, Worcester, MA 01606<br>ATTN: Dr. N. Ault<br>Dr. M. L. Torti   |
| 1             | AVCO Corporation, Applied Technology Division, Lowell Industrial Park, Lowell, MA 01887<br>ATTN: Dr. T. Vasilos   | 1             | Pennsylvania State University, Materials Research Laboratory, Materials Science Department, University Park, PA 16802<br>ATTN: Prof. R. E. Tressler<br>Prof. R. Bradt<br>Prof. V. S. Stubican |
| 1             | Carborundum Company, Research and Development Division, P.O. Box 1054, Niagara Falls, NY 14302<br>ATTN: Dr. J. A. Coppola   | 1             | RIAS, Division of the Martin Company, Baltimore, MD 21203<br>ATTN: Dr. A. R. C. Westwood  |
| 1             | Case Western Reserve University, Department of Metallurgy, Cleveland, OH 44106<br>ATTN: Prof. A. H. Heuer   | 1             | Rockwell International Corporation, Science Center, 1049 Camino Dos Rios, Thousand Oaks, CA 91360<br>ATTN: Dr. F. F. Lange  |
| 1             | Cummins Engine Company, Columbus, IN 47201<br>ATTN: Mr. R. Kamo   | 1             | Stanford Research International, 333 Ravenswood Avenue, Menlo Park, CA 94025<br>ATTN: Dr. P. Jorgensen<br>Dr. D. Rowcliffe  |
| 1             | Deposits and Composites, Inc., 318 Victory Drive, Herndon, VA 22070<br>ATTN: Mr. R. E. Engdahl  | 1             | State University of New York at Stony Brook, Department of Materials Science, Long Island, NY 11790<br>ATTN: Prof. Franklin F. Y. Wang  |
| 1             | Electric Power Research Institute, P.O. Box 10412, 3412 Hillview Avenue, Palo Alto, CA 94304<br>ATTN: Dr. A. Cohn   | 1             | United Technologies Research Center, East Hartford, CT 06108<br>ATTN: Dr. J. Brennan<br>Dr. F. Galasso  |
| 1             | European Research Office, 223 Old Marylebone Road, London, NW1 - 5th, England<br>ATTN: Dr. R. Quattrone<br>LT COL James Kennedy   | 1             | University of California, Lawrence Livermore Laboratory, P.O. Box 808, Livermore, CA 94550<br>ATTN: Dr. C. F. Cline   |
| 1             | Ford Motor Company, Turbine Research Department, 20000 Rotunda Drive, Dearborn, MI 48121<br>ATTN: Mr. A. F. McLean<br>Mr. E. A. Fisher<br>Mr. J. A. Mangels                       | 1             | University of Florida, Department of Materials Science and Engineering, Gainesville, FL 32601<br>ATTN: Dr. L. Hench   |
| 1             | General Electric Company, Research and Development Center, Box 8, Schenectady, NY 12345<br>ATTN: Dr. R. J. Charles<br>Dr. C. D. Greskovich<br>Dr. S. Prochazka                    | 1             | University of Michigan, Materials of Metallurgical Engineering, Ann Arbor, MI 48104<br>ATTN: Prof. E. E. Huckle<br>Prof. T. Y. Tien   |
| 1             | General Motors Corporation, AC Spark Plug Division, Flint, MI 48556<br>ATTN: Mr. Fred Kennard   | 1             | University of Newcastle Upon Tyne, Department of Metallurgy and Engineering Materials, Newcastle Upon Tyne, NE1 7 PU, England<br>ATTN: Prof. K. H. Jack                                       |
| 1             | Georgia Institute of Technology, EES, Atlanta, GA 30332<br>ATTN: Mr. J. D. Walton   | 1             | University of Washington, Ceramic Engineering Division, FB-10, Seattle, WA 98195<br>ATTN: Prof. James I. Mueller<br>Prof. A. Miller   |
| 1             | GTE Laboratories, Waltham Research Center, 40 Sylvan Road, Waltham, MA 02154<br>ATTN: Dr. C. Quackenbush<br>Dr. W. H. Rhodes<br>Dr. J. T. Smith                                   | 1             | Virginia Polytechnic Institute, Department of Materials Engineering, Blacksburg, VA 24061<br>Prof. D. P. H. Hasselman   |
| 1             | IIT Research Institute, 10 West 35th Street, Chicago, IL 60616<br>ATTN: Mr. S. Bortz, Director, Ceramics Research   | 1             | Westinghouse Electric Corporation, Research Laboratories, Pittsburgh, PA 15235<br>ATTN: Dr. R. J. Bratton   |
| 1             | Institut fur Werkstoff-Forschung, DFVLR, 505 Porz-Wahn, Linder Hohe, Germany<br>ATTN: Dr. W. Bunk   | 1             | Mr. Joseph T. Bailey, 3M Company, Technical Ceramic Products Division, 3M Center, Building 207-1W, St. Paul, MN 55101   |
| 1             | Caterpillar Tractor Co., Solar Division, 2200 Pacific Highway, P.O. Box 80966, San Diego, CA 92138<br>ATTN: Dr. A. Metcalfe<br>Ms. M. E. Gulden                                   | 1             | Dr. Jacob Stiglich, Dart Industries/San Fernando Laboratories, 10258 Norris Avenue, Pacoima, CA 91331   |
| 1             | Kawecik Berylco Industries, Inc., P.O. Box 1462, Reading, PA 19603<br>ATTN: Mr. R. J. Longenecker   | 1             | Dr. J. Petrovic - CMB-5, Mail Stop 730, Los Alamos Scientific Laboratories, Los Alamos, NM 87545  |
| 1             | Martin Marietta Laboratories, 1450 South Rolling Road, Baltimore, MD 21227<br>ATTN: Dr. J. Venables   | 1             | Mr. R. J. Zentner, EAI Corporation, 198 Thomas Johnson Drive, Suite 16, Frederick, MD 21701   |
| 1             | Massachusetts Institute of Technology, Department of Metallurgy and Materials Science, Cambridge, MA 02139<br>ATTN: Prof. R. L. Coble<br>Prof. H. K. Bowen<br>Prof. W. D. Kingery | 2             | Director, Army Materials and Mechanics Research Center, Watertown, MA 02172<br>ATTN: DRXMR-PL<br>DRXMR-PAT<br>DRXMR-K<br>DRXMR-MC, Mr. G. E. Gazza  |

|   |   |
|---|---|
| <p>Army Materials and Mechanics Research Center<br/>Watertown, Massachusetts 02172<br/>DEVELOPMENT OF SINTERED <math>\text{Si}_3\text{N}_4</math> FOR HIGH PERFORMANCE THERMOMECHANICAL APPLICATIONS<br/>W.D. Pasco<br/>General Electric Company<br/>Corporate Research and Development<br/>Schenectady, New York 12301</p> <p>AD _____</p> <p>UNCLASSIFIED<br/>UNLIMITED DISTRIBUTION</p> <p>Key Words<br/>Sintering<br/>Silicon Nitrides<br/>Beryllium Compounds<br/>Yttrium Oxides<br/>High Temperature<br/>Ceramics Materials</p> <p>Technical Report AMMRC-TR84-4, January 1984<br/>56 pp.-illus.-tables, Contract DAAG46-82-C-0058<br/>Final Report, August 1982 - August 1983</p> <p>The sintering of <math>\text{Si}_3\text{N}_4</math>, containing BeSiN<sub>2</sub> and <math>\text{Y}_2\text{O}_3</math>, was examined and found to yield densities greater than 98% on a routine basis. A composition containing 2.5 wt% BeSiN<sub>2</sub> and 3.0 wt% <math>\text{Y}_2\text{O}_3</math> displayed a room temperature strength of greater than 690 MPa and a fracture toughness <math>K_{IC}</math> of about 6 MNm<sup>-3/2</sup>, a creep rate of <math>4 \times 10^{-11}</math> h<sup>-1</sup> at 1300 °C under a 69 MPa load, and a parabolic rate constant for oxidation at 1350 °C of <math>1.7 \times 10^{-11}</math> kg<sup>2</sup>m<sup>-3</sup>s<sup>-1</sup>. This composition has adequate properties for high temperature structural applications except for the high creep rate, which is of the same order as NC-132.</p> <p>The sintering of <math>\text{Si}_3\text{N}_4</math>, containing 5 wt% LiAlO<sub>2</sub> and 3 wt% YF<sub>3</sub>, was examined and found to yield densities of greater than 96%. The creep rate of this composition was <math>5 \times 10^{-10}</math> h<sup>-1</sup> at 1300 °C under a 69 MPa load. The high creep rate, in conjunction with a moderately high oxidation rate, precludes the use of this composition for high temperature structural applications.</p> <p>A new source of <math>\text{Si}_3\text{N}_4</math> powder, made by Ube Industries, was qualified as an alternative powder source of this program. The addition of 7 wt% BeSiN<sub>2</sub>, in conjunction with a total oxygen content of 3.5 wt% yielded sintered densities of greater than 98.5%.</p> | <p>Army Materials and Mechanics Research Center<br/>Watertown, Massachusetts 02172<br/>DEVELOPMENT OF SINTERED <math>\text{Si}_3\text{N}_4</math> FOR HIGH PERFORMANCE THERMOMECHANICAL APPLICATIONS<br/>W.D. Pasco<br/>General Electric Company<br/>Corporate Research and Development<br/>Schenectady, New York 12301</p> <p>AD _____</p> <p>UNCLASSIFIED<br/>UNLIMITED DISTRIBUTION</p> <p>Key Words<br/>Sintering<br/>Silicon Nitrides<br/>Beryllium Compounds<br/>Yttrium Oxides<br/>High Temperature<br/>Ceramics Materials</p> <p>Technical Report AMMRC-TR84-4, January 1984<br/>56 pp.-illus.-tables, Contract DAAG46-82-C-0058<br/>Final Report, August 1982 - August 1983</p> <p>The sintering of <math>\text{Si}_3\text{N}_4</math>, containing BeSiN<sub>2</sub> and <math>\text{Y}_2\text{O}_3</math>, was examined and found to yield densities greater than 98% on a routine basis. A composition containing 2.5 wt% BeSiN<sub>2</sub> and 3.0 wt% <math>\text{Y}_2\text{O}_3</math> displayed a room temperature strength of greater than 690 MPa and a fracture toughness <math>K_{IC}</math> of about 6 MNm<sup>-3/2</sup>, a creep rate of <math>4 \times 10^{-11}</math> h<sup>-1</sup> at 1300 °C under a 69 MPa load, and a parabolic rate constant for oxidation at 1350 °C of <math>1.7 \times 10^{-11}</math> kg<sup>2</sup>m<sup>-3</sup>s<sup>-1</sup>. This composition has adequate properties for high temperature structural applications except for the high creep rate, which is of the same order as NC-132.</p> <p>The sintering of <math>\text{Si}_3\text{N}_4</math>, containing 5 wt% LiAlO<sub>2</sub> and 3 wt% YF<sub>3</sub>, was examined and found to yield densities of greater than 96%. The creep rate of this composition was <math>5 \times 10^{-10}</math> h<sup>-1</sup> at 1300 °C under a 69 MPa load. The high creep rate, in conjunction with a moderately high oxidation rate, precludes the use of this composition for high temperature structural applications.</p> <p>A new source of <math>\text{Si}_3\text{N}_4</math> powder, made by Ube Industries, was qualified as an alternative powder source of this program. The addition of 7 wt% BeSiN<sub>2</sub>, in conjunction with a total oxygen content of 3.5 wt% yielded sintered densities of greater than 98.5%.</p> |
|---|---|

|   |   |
|---|---|
| <p>Army Materials and Mechanics Research Center<br/>Watertown, Massachusetts 02172<br/>DEVELOPMENT OF SINTERED <math>\text{Si}_3\text{N}_4</math> FOR HIGH PERFORMANCE THERMOMECHANICAL APPLICATIONS<br/>W.D. Pasco<br/>General Electric Company<br/>Corporate Research and Development<br/>Schenectady, New York 12301</p> <p>AD _____</p> <p>UNCLASSIFIED<br/>UNLIMITED DISTRIBUTION</p> <p>Key Words<br/>Sintering<br/>Silicon Nitrides<br/>Beryllium Compounds<br/>Yttrium Oxides<br/>High Temperature<br/>Ceramics Materials</p> <p>Technical Report AMMRC-TR84-4, January 1984<br/>56 pp.-illus.-tables, Contract DAAG46-82-C-0058<br/>Final Report, August 1982 - August 1983</p> <p>The sintering of <math>\text{Si}_3\text{N}_4</math>, containing BeSiN<sub>2</sub> and <math>\text{Y}_2\text{O}_3</math>, was examined and found to yield densities greater than 98% on a routine basis. A composition containing 2.5 wt% BeSiN<sub>2</sub> and 3.0 wt% <math>\text{Y}_2\text{O}_3</math> displayed a room temperature strength of greater than 690 MPa and a fracture toughness <math>K_{IC}</math> of about 6 MNm<sup>-3/2</sup>, a creep rate of <math>4 \times 10^{-11}</math> h<sup>-1</sup> at 1300 °C under a 69 MPa load, and a parabolic rate constant for oxidation at 1350 °C of <math>1.7 \times 10^{-11}</math> kg<sup>2</sup>m<sup>-3</sup>s<sup>-1</sup>. This composition has adequate properties for high temperature structural applications except for the high creep rate, which is of the same order as NC-132.</p> <p>The sintering of <math>\text{Si}_3\text{N}_4</math>, containing 5 wt% LiAlO<sub>2</sub> and 3 wt% YF<sub>3</sub>, was examined and found to yield densities of greater than 96%. The creep rate of this composition was <math>5 \times 10^{-10}</math> h<sup>-1</sup> at 1300 °C under a 69 MPa load. The high creep rate, in conjunction with a moderately high oxidation rate, precludes the use of this composition for high temperature structural applications.</p> <p>A new source of <math>\text{Si}_3\text{N}_4</math> powder, made by Ube Industries, was qualified as an alternative powder source of this program. The addition of 7 wt% BeSiN<sub>2</sub>, in conjunction with a total oxygen content of 3.5 wt% yielded sintered densities of greater than 98.5%.</p> | <p>Army Materials and Mechanics Research Center<br/>Watertown, Massachusetts 02172<br/>DEVELOPMENT OF SINTERED <math>\text{Si}_3\text{N}_4</math> FOR HIGH PERFORMANCE THERMOMECHANICAL APPLICATIONS<br/>W.D. Pasco<br/>General Electric Company<br/>Corporate Research and Development<br/>Schenectady, New York 12301</p> <p>AD _____</p> <p>UNCLASSIFIED<br/>UNLIMITED DISTRIBUTION</p> <p>Key Words<br/>Sintering<br/>Silicon Nitrides<br/>Beryllium Compounds<br/>Yttrium Oxides<br/>High Temperature<br/>Ceramics Materials</p> <p>Technical Report AMMRC-TR84-4, January 1984<br/>56 pp.-illus.-tables, Contract DAAG46-82-C-0058<br/>Final Report, August 1982 - August 1983</p> <p>The sintering of <math>\text{Si}_3\text{N}_4</math>, containing BeSiN<sub>2</sub> and <math>\text{Y}_2\text{O}_3</math>, was examined and found to yield densities greater than 98% on a routine basis. A composition containing 2.5 wt% BeSiN<sub>2</sub> and 3.0 wt% <math>\text{Y}_2\text{O}_3</math> displayed a room temperature strength of greater than 690 MPa and a fracture toughness <math>K_{IC}</math> of about 6 MNm<sup>-3/2</sup>, a creep rate of <math>4 \times 10^{-11}</math> h<sup>-1</sup> at 1300 °C under a 69 MPa load, and a parabolic rate constant for oxidation at 1350 °C of <math>1.7 \times 10^{-11}</math> kg<sup>2</sup>m<sup>-3</sup>s<sup>-1</sup>. This composition has adequate properties for high temperature structural applications except for the high creep rate, which is of the same order as NC-132.</p> <p>The sintering of <math>\text{Si}_3\text{N}_4</math>, containing 5 wt% LiAlO<sub>2</sub> and 3 wt% YF<sub>3</sub>, was examined and found to yield densities of greater than 96%. The creep rate of this composition was <math>5 \times 10^{-10}</math> h<sup>-1</sup> at 1300 °C under a 69 MPa load. The high creep rate, in conjunction with a moderately high oxidation rate, precludes the use of this composition for high temperature structural applications.</p> <p>A new source of <math>\text{Si}_3\text{N}_4</math> powder, made by Ube Industries, was qualified as an alternative powder source of this program. The addition of 7 wt% BeSiN<sub>2</sub>, in conjunction with a total oxygen content of 3.5 wt% yielded sintered densities of greater than 98.5%.</p> |
|---|---|

END

FILMED

6-34

DTIC